GUGGENHEIM AERONAUTICAL LABORATORY

CALIFORNIA INSTITUTE OF TECHNOLOGY

FLOW FIELD AROUND A FINITE CONE WITH SHOCK

Thesis by

Lt. Comdr. V. U. Muirhead

1949

PASADENA, CALIFORNIA

FLOW FIELD AROUND A FINITE CONE WITH SHOCK

Thesis by

Lt. Comdr. Vincent Uriel Muirhead, USN

In Partial Fulfillment of the Requirements

for the Degree of Aeronautical Engineer

California Institute of Technology

Pasadena, California

1949

ABSTRACT

The objective of this investigation was to study the flow field in the immediate vicinity of a finite cone and to compare the results with analytical values for an infinite cone. Pressure distribution over the surface of a 70° cone and the general characteristics of the shock wave were investigated. The tests were conducted at five Mach numbers covering the four regimes of flow. Particular attention was given to the conditions at the apex of the cone. The locations of the intersection of the sonic line with the surface of the cone and with the shock wave were determined.

In general the tests demonstrate that at the apex of a finite cone the pressure and the shock wave angle closely approach the values predicted by analytical methods in the four regimes of flow.

The tests were conducted in the GALCIT 2.5" Supersonic Wind Tunnel.

ACKNOWLEDGMENTS

This investigation was conducted jointly with Mr. Neil Mac Kinnon. Appreciation is expressed to Mr. Allen R. Puckett and Mr. Henry Nagamatsu for their advice and assistance.

TABLE OF CONTENTS

LIST OF FIGURES

LIST OF FIGURES

I. INTRODUCTION

The objective of this investigation was to study the flow field in the immediate vicinity of a finite cone and to compare the results with analytical values for an infinite cone. A previous investigation was made by Marschner (Ref. 1). The results of this were inconclusive for conditions near the apex of the cone at Mach numbers near the attachment Mach number. Also, because of the selection of the cone angle, his results were not directly comparable to the analytical solutions by Kopal (Ref. 2).

This investigation was made on a circular cylinder with a 70° conical nose since this was one of the cone angles for which the tabular solution was available in (Ref. 2). The pressure distribution over the surface of the cone and the general characteristics of the shock wave at each flow condition were investigated. The location of the points at which the local Mach number became one, both on the surface of the cone and immediately behind the shock wave, were determined. Particular attention was given to conditions close to the apex of the cone. This was accomplished by the use of a diameter for the cylinder just slightly smaller than the blocking size for the tunnel at the lowest test Mach number, and by the use of a pressure orifice as close as possible to the apex of the cone. Five test Mach numbers were selected in order that the flow over the cone could be investigated in all four regimes: detached shock with subsonic flow between the shock wave and the cone, attached shock with subsonic flow

between the shock wave and the cone, attached shock with mixed flow between the shock wave and the cone, and attached shock with supersonic flow between the shock wave and the cone. Two of the test Mach numbers were close to the attachment Mach number. The Mach numbers selected to cover the four regimes were: 1.49, 1.636, 1.694, 1.86, and 1.997.

Theoretical results for infinite cones have been tabulated by Kopal (Ref. 2). These analytical results show for the 70° infinite cone that:

Initial Mach Number	Wave Position	Mach Number After Shock	Surface Mach Number
$1.000 < M < 1.681$	Detached	Subsonic	Subsonic
$1.681 < M < 1.769$	Attached	Subsonic	Subsonic
$1.769 < M < 1.911$	Attached	Supersonic	Subsonic
$1.911 < M < \infty$	Attached	Supersonic	Supersonic

II. EQUIPMENT AND PROCEDURE

The models used for this investigation were machined from brass with an apex angle of 70°. The cylinder diameter selected was .5 inches to obtain a size which would furnish the largest conical surface but which would not block the tunnel at Mach number of 1.49. A series of eight models were used in order to make pressure measurements on the surface of the cone and behind the shoulder. Each model has a pressure orifice located on the cone, as shown in Fig. 1. Other than the location of the pressure orifice the models were identical. The number one orifice was placed as close to the apex as possible; the others were spaced over the remaining conical surface and behind the shoulder.

The wind tunnel used for the tests was the GALCIT Supersonic Wind Tunnel. The tunnel is of closed throat, rectangular cross-section, single return type. The test section is 2.5" by 2.5". Complete details of the tunnel are given in GALCIT publication (Ref. 3). For two of the tests, Mach numbers 1.636 and 1.997, fixed nozzle blocks were used. A flexible nozzle was used to obtain the other three Mach numbers: 1.49, 1.694, and 1.86. A description of the flexible nozzle and adjusting equipment is outlined in (Ref. 1). Each nozzle was calibrated by an axial static tube. The results of these calibrations are shown in Fig. 2.

Pressure data was measured on each of the eight models at each Mach number by the use of mercury U-tube manometers. All measurements were made at zero angle of attack relative to the flow. The zero angle was

determined for each model for every test. The procedure followed for this was to place the orifice of the model in an up position and measure the pressure for several angles of attack relative to an arbitrary zero. The orifice was then placed in a down position and the pressures measured at these same angles. From a plot of these the zero angle of attack relative to the flow was determined. A sample plot of this procedure is shown in Fig. 3. The model was then set to this position and the orifice pressure checked with the orifice in both positions.

With the model at zero angle of attack, a Schlieren picture was taken. The orifice pressure, the wind tunnel settling tank stagnation pressure, and a representative test section wall orifice pressure were recorded. Throughout the tests the relative humidity of the tunnel was maintained between two and four per cent by the dryer.

III. RESULTS AND DISCUSSION

In Fig. 4 are given the symbols used in the reduction and presentation of data. The pressure measurements obtained were reduced to non-dimensional form, P_s/P_o, P_s being the particular orifice pressure and P_o, the stagnation pressure in the settling chamber of the tunnel. Fig. 5 through 9 show the results for each Mach number of P_s/P_o plotted against s/x. x/s is the distance of the particular orifice from the apex of the cone divided by the slant distance of the surface of the cone. In Fig. 10 is a summary of this data. The variation of P_s/P_o for each orifice with Mach number is shown in Fig. 11.

The pressure measurements were also reduced to the non-dimensional form of P_s/P_o', P_o' being the reservoir pressure behind the shock wave at the apex. For Mach numbers of 1.49 and 1.636 the normal shock wave relations were used to determine P_o'. The oblique shock wave relations were used to determine P_o' for Mach numbers with attached shock wave. Fig. 12 through 16 show P_s/P_o' plotted against x/s, with a summary in Fig. 17. The variation of P_s/P_o' with Mach number is shown in Fig. 18.

The Schlieren negatives were projected and the wave angles measured at various stations from the centerline of the cone. In Fig. 19 the shock wave pattern is shown six times actual size. In Figs. 20 through 24 is plotted the variation of the wave angle, θ_w, with Y/D, Y being the distance from the centerline of the cone and D, the cylinder diameter. From the angles the Mach number, M_2, behind

the wave was computed by the oblique shock wave theory and plotted. A summary of θ_w and M_2 is shown in Figs. 25 and 26.

For the Mach numbers of 1.49 and 1.636, the stagnation pressures behind the shock were computed from the normal shock relations. These were plotted in Figs. 5 and 6. It is seen from the test data that the surface pressures for these two cases increase toward the apex of the cone and tend to approach the stagnation pressure. From the stagnation pressure behind the shock, the pressure for M = 1 was computed and plotted at x/s = 1 in the figures. The tests show reasonable agreement with these analytical values.

From Kopal (Ref. 2), a theoretical curve of P_s/P_o with Mach number for the 70° infinite cone was made in Fig. 27. The values of P_s/P_o for M = 1.694, 1.86, and 1.997 from this curve were plotted in Figs. 7, 8, and 9. In each case the test results show that the surface pressure closely approached the analytical values at the apex of the cone. From P_o' the value of P_s/P_o for M = 1 was computed and plotted for M = 1.694 and 1.86. At M = 1.694 it appears that a local Mach number of one is reached at an x/s of .975. At M = 1.86 this value is reached at an x/s of .5. These tests indicate that the point, at which the local Mach number reached one, moves down the surface of the cone from the shoulder toward the apex as the Mach number increases, until the whole region is supersonic. Using the Prandtl-Meyer expansion relations, the pressure at the shoulder of the cone was computed and plotted in Fig. 9 for M = 1.997.

In Figs. 21 and 22 is shown the fact that the shock angle approaches the normal shock at the centerline of the cone for the detached cases.

M_2 reached one at a Y/D of .96 for M = 1.49, and at .83 for M = 1.636. A theoretical curve of the shock wave angle, θ_w, with Mach number for the 70° infinite cone was drawn in Fig. 28 from (Ref. 2). These values for the three attached shock waves were plotted in Figs. 23, 24, and 25. From these it is seen that the measured wave angle at the apex was in close agreement with the analytical results. For the test Mach number of 1.694, M_2 equaled 1 at a Y/D of .67. For the Mach numbers of 1.86 and 1.997, M_2 was at all points supersonic. In Figs. 29 through 35 are representative Schlieren photographs taken during the tests.

The results of these tests are in agreement with the results obtained in (Ref. 1). The patterns of the pressure distribution curves exhibit the same general characteristics. In both there is a gradual decrease in the slope and lowering of the pressure curves for both the detached and the attached conditions, with an increase in Mach number.

Within the scope of this investigation, the results indicate that the pressure and shock wave angle at the apex of the 70° finite cone closely approach the analytical results for the 70° infinite cone. The conditions near the region of the attachment Mach number which were open to question from the results obtained in (Ref. 1) now appear to follow the detached condition until the attachment Mach number is reached. After attachment, the analytical conical flow solution predicts the apex conditions.

IV. CONCLUSIONS

In general the tests demonstrate that the surface pressure and the shock wave angle closely approach the values predicted by the analytical methods in the four regimes of flow only at the apex of a finite cone. For the mixed flow regimes, that is when the Mach number behind the shock wave at some point was less than one, the flow is non-conical. When the Mach number behind the shock is greater than one, the flow is practically conical.

By extension, it is therefore indicated that the analytical results obtained from (Ref. 2) for flow conditions other than those tested would be in reasonable agreement with test results.

REFERENCES

1. Marschner, Bernard W., "An Investigation of Detached Shock Waves", Thesis, California Institute of Technology, 1948.

2. Kopal, Z., "Supersonic Flow Around Cones", Massachusetts Institute of Technology, Center of Analysis, Report No. 1, 1947.

3. Puckett, Allen E. and Schamberg, Richard, "Final Report - Galcit Supersonic Wind Tunnel Tests", Library of Aeronautics, California Institute of Technology, June, 1946.

SAMPLE CALCULATIONS

A. Determination of M

Data:

z	P_o	P_A	P_4	P_A	P_s	P_4	Baro
5/8"	102.6	99.2	132.65	70.35	63.30	5.84	74.70

P_o	102.6	P_4	132.65
P_A	99.2	P_A	70.35
	3.4		62.30
Baro	74.7	Baro	74.70
	3.4		62.30
P_o =	71.3	P_4 =	12.40

$$\frac{P_4}{P_o} = \frac{12.4}{71.3} = .1739$$

$$\frac{.2188\ (P_4 - P_s)}{P_o} = \frac{.2188\ (58.4 - 63.3)}{71.3} = -.01504$$

$$\frac{P_s}{P_o} = .1739 - .0150 = .1575$$

$$M = 1.860$$

B. Determination of Angle of Attack

Data:

	Rel. Angle	P_s	P_A	ΔP
Hole up	0	112.70	92.10	20.60
Hole up	1.0	112.90	91.85	21.05
Hole down	0	112.90	91.85	21.05
Hole down	1.0	112.65	92.15	20.50

C. Determination of P_s/P_o; M = 1.86

Data:

Run	Model	P_o	P_A	Baro	P_s	P_A	P_4	P_A	T
52	3	102.65	99.15	74.88	121.6	81.6	75.45	13.35	23.3

P_o	102.65	P_s	121.6
P_A	99.15	P_A	81.8
	3.50		39.8
Baro	74.88	Baro	74.88
	3.50		39.8
P_o =	71.38	P_s =	35.08

$$P_s/P_o = \frac{35.08}{71.38} = .4915$$

D. Determination of P_s/P_o'; M = 1.86

$$\frac{P_o}{P_o'} = \left(\frac{2.8}{2.4} M^2 \sin^2 \theta_w - \frac{.4}{2.4}\right)^{2.5} \left(\frac{.2\, M^2 \sin^2 \theta_w + 1}{1.2\, M^2 \sin^2 \theta_w}\right)^{3.5}$$

$$= \left(\frac{2.8}{2.4} (1.86)^2 (\sin 58.2)^2 - \frac{.4}{2.4}\right)^{2.5} \left(\frac{.2(1.86)^2 (\sin 58.2)^2 + 1}{1.2(1.86)^2 (\sin^2 58.2)^2}\right)^{3.5}$$

$$= 1.108$$

$$\frac{P_s}{P_o'} = \frac{P_s}{P_o'} \times \frac{P_o}{P_o'} = .491 \times 1.108 = .544$$

E. Determination of M = 1 on cone

$$\left(\frac{P_s}{P_o}\right)_{M=1} = .528 \frac{P_o'}{P_o} = \frac{.528}{1.108} = .477$$

F. Determination of P_s/P_o (Kopal theoretical)

$$\frac{P_s}{P_o} = \frac{P_s}{P_w} \times \frac{P_w}{P_1} \times \frac{P_1}{P_o}$$

$$\frac{P_s}{P_o} = 1.1475 \times 2.74 \times 1.58 = .497$$

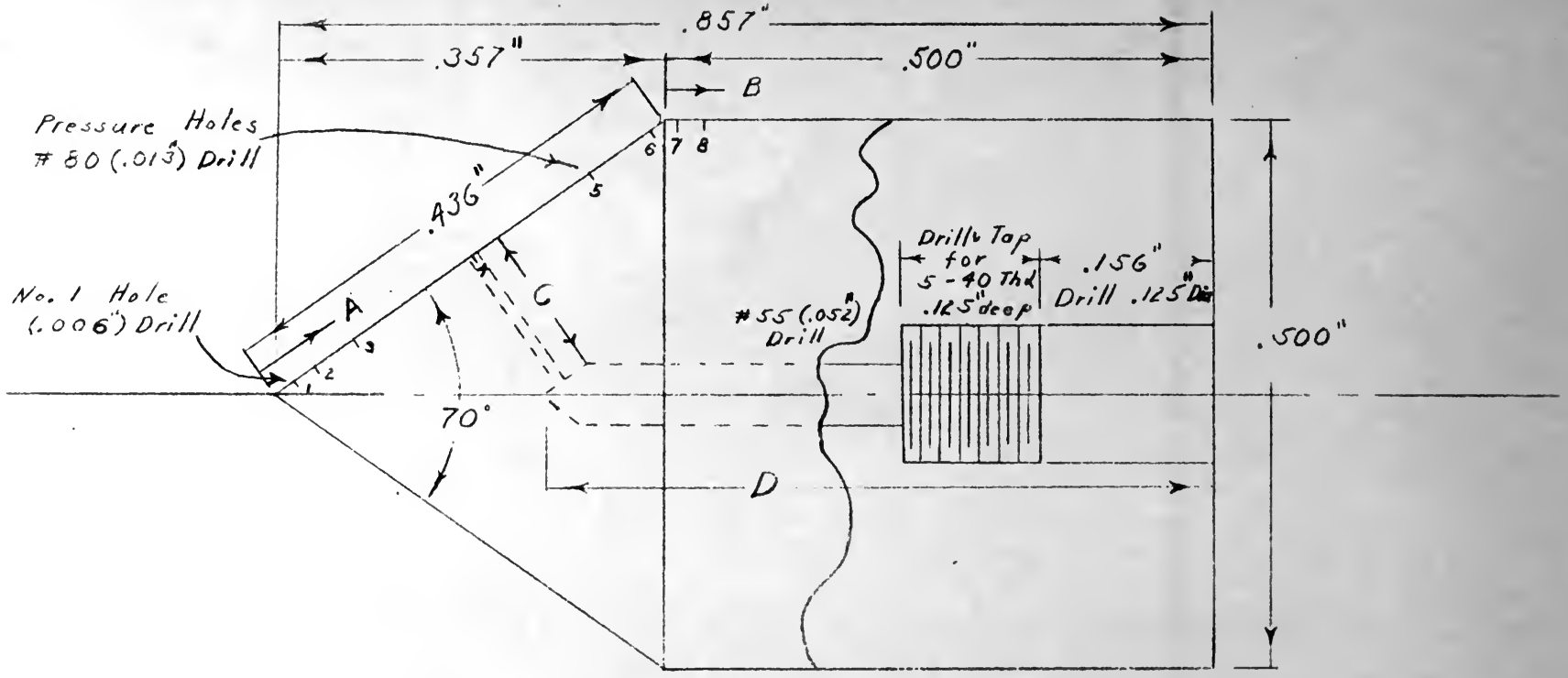

Scale 6" = 1"

Cone #	A	B	C	D
1	.019"		.014"	.840"
2	.044"		.031"	.803"
3	.088"		.061"	.751"
4	.218"		.153"	.591"
5	.350"		.245"	.431"
6	.425"		.299"	.337"
7		.0114"	.255"	.987"
8		.0355"	.255"	.464"

Fig. 1
Cone Pressure
Models

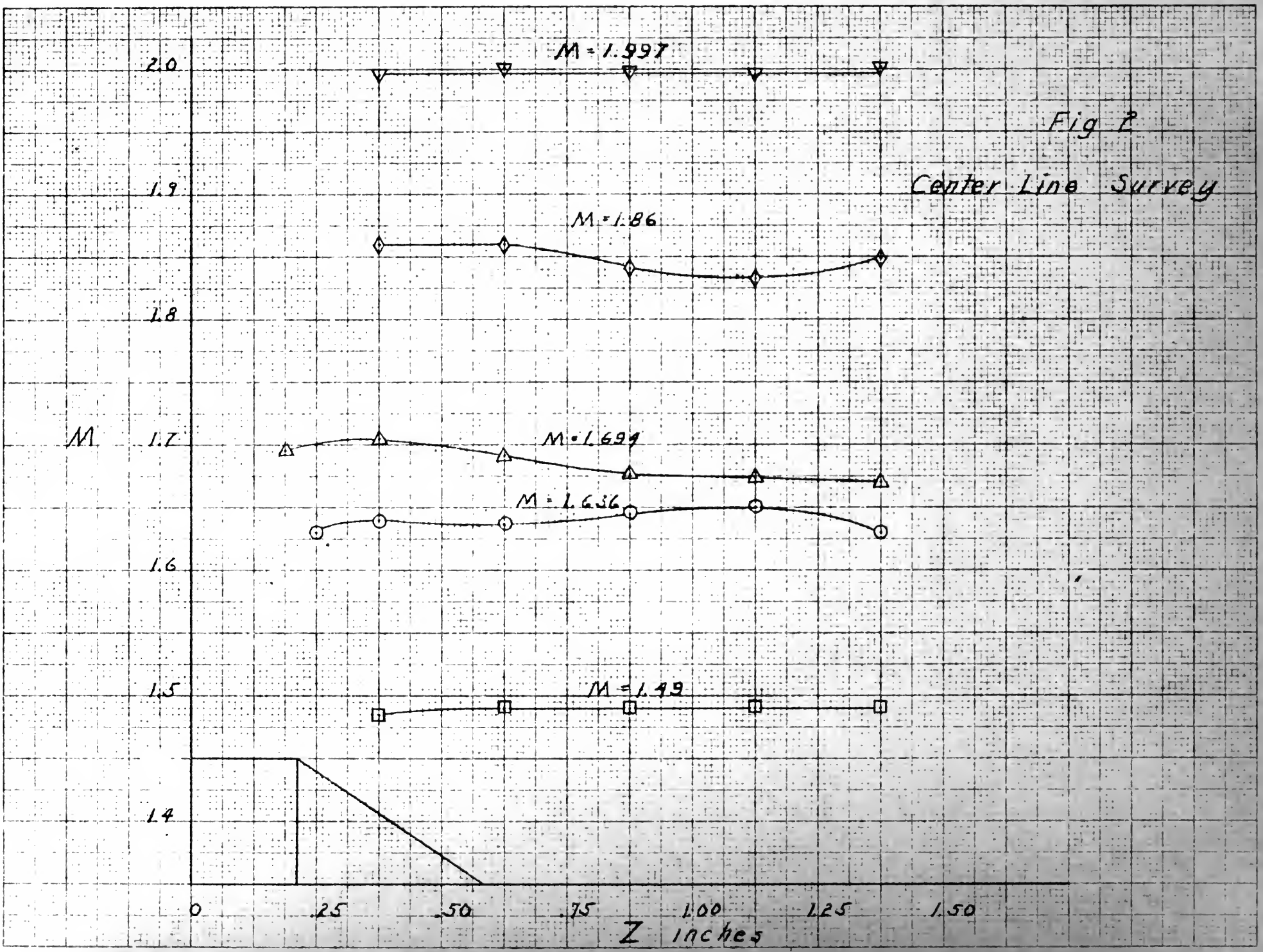

Fig 2

Center Line Survey

Fig 3 Determination of Angle of Attack

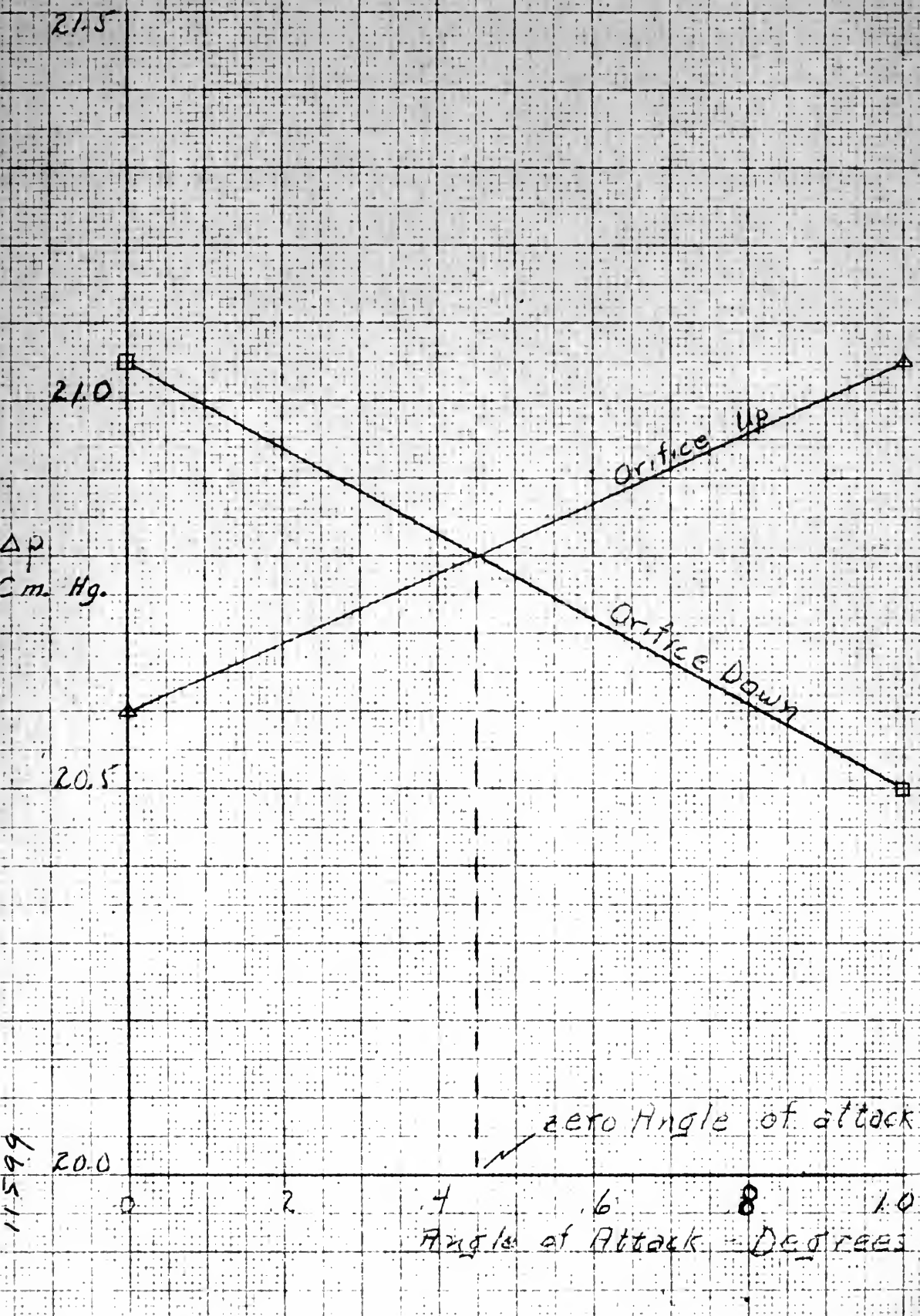

Fig. 4 Symbols

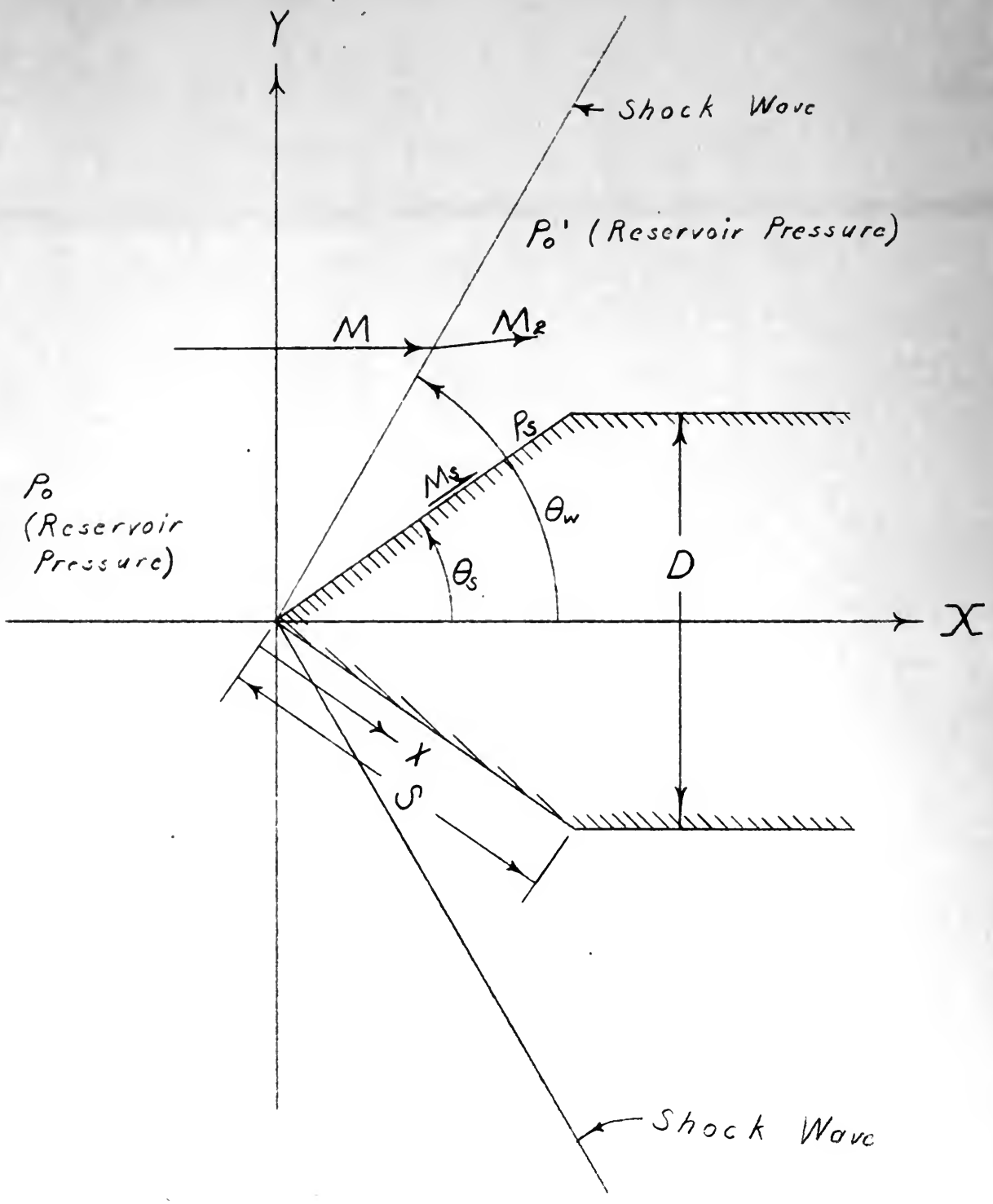

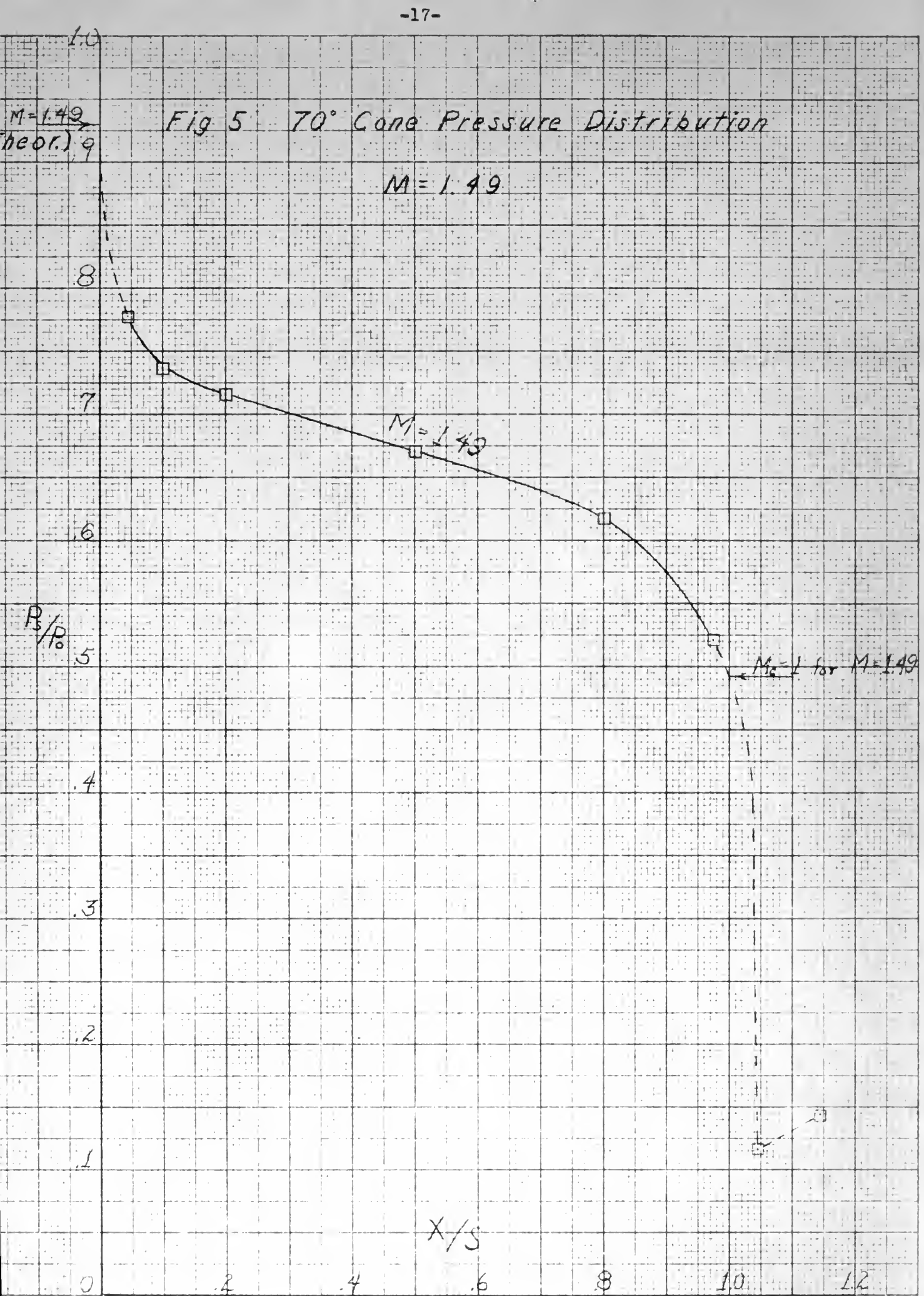

Fig 5 70° Cone Pressure Distribution

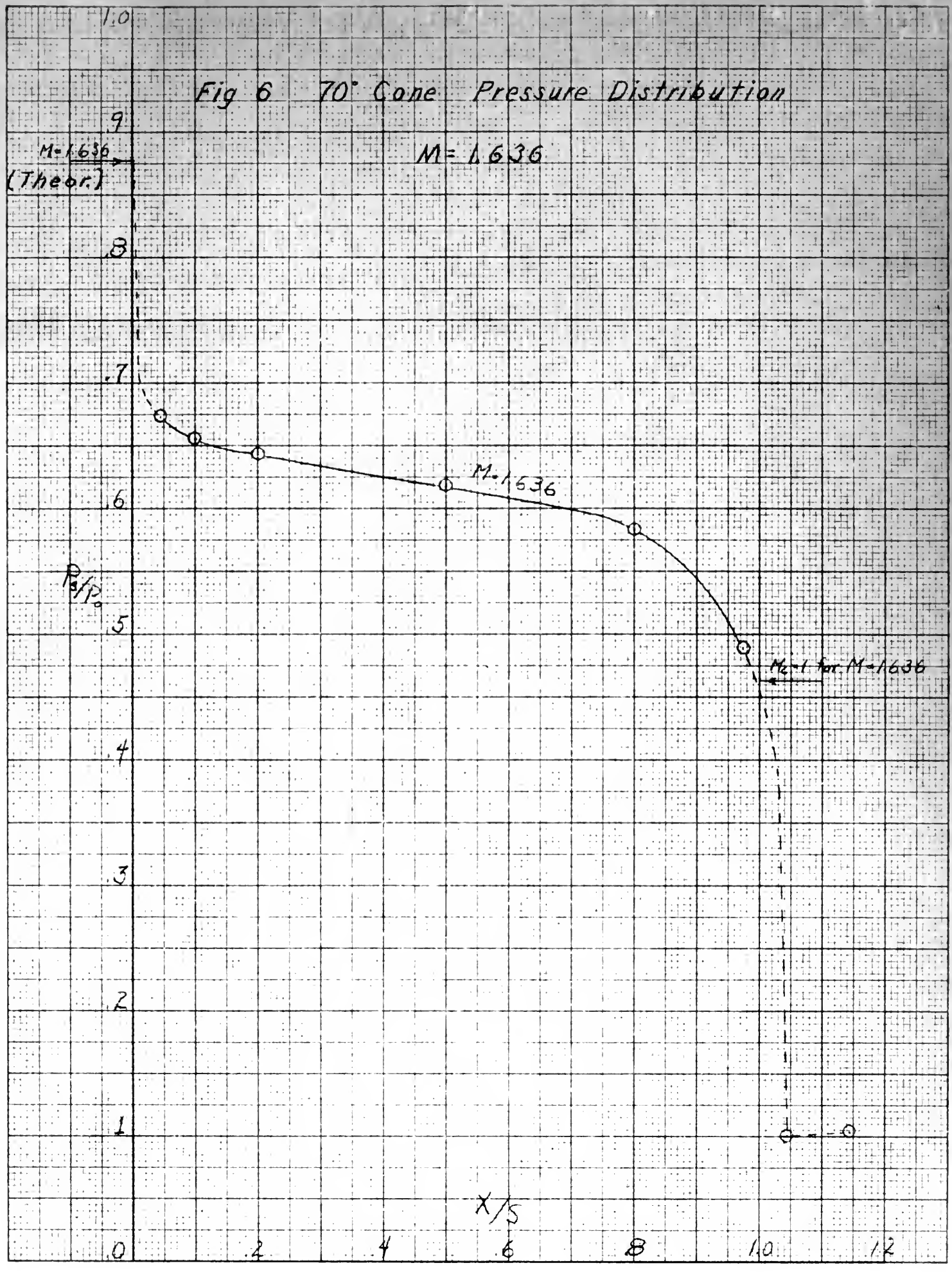
Fig 6 70° Cone Pressure Distribution
M = 1.636
M=1.636 (Theor.)
M=1.636
M2=1 for M=1.636
Ps/P0
X/S
1.0
.9
.8
.7
.6
.5
.4
.3
.2
.1
0
.2
.4
.6
.8
1.0
1.2

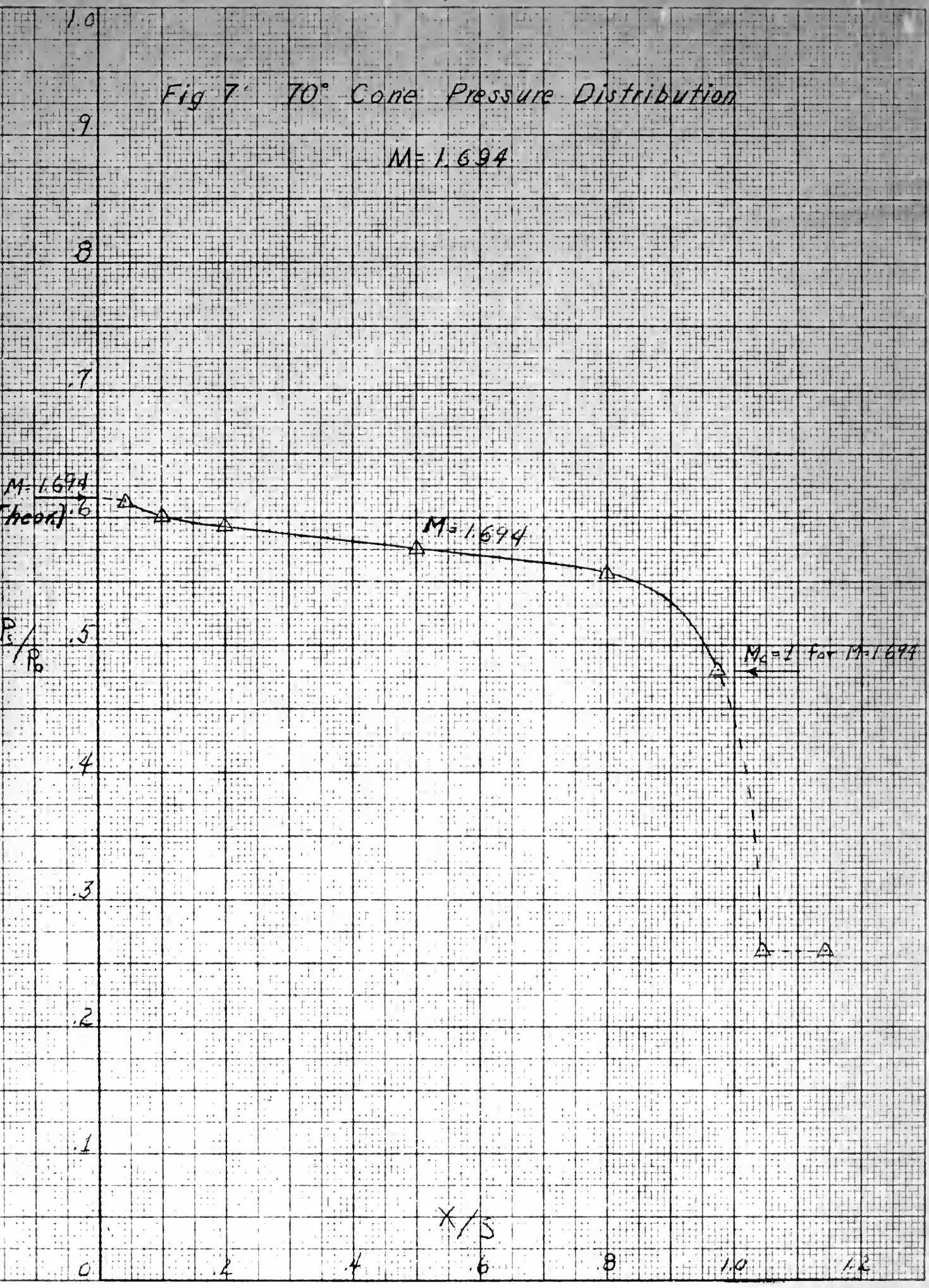
Fig 7 70° Cone Pressure Distribution
M=1.694
M=1.694 (theor.)
M=1.694
Mc=1 for M=1.694
Pc/Pb
X/S
1.0
.9
.8
.7
.6
.5
.4
.3
.2
.1
0
.2
.4
.6
.8
1.0
1.2

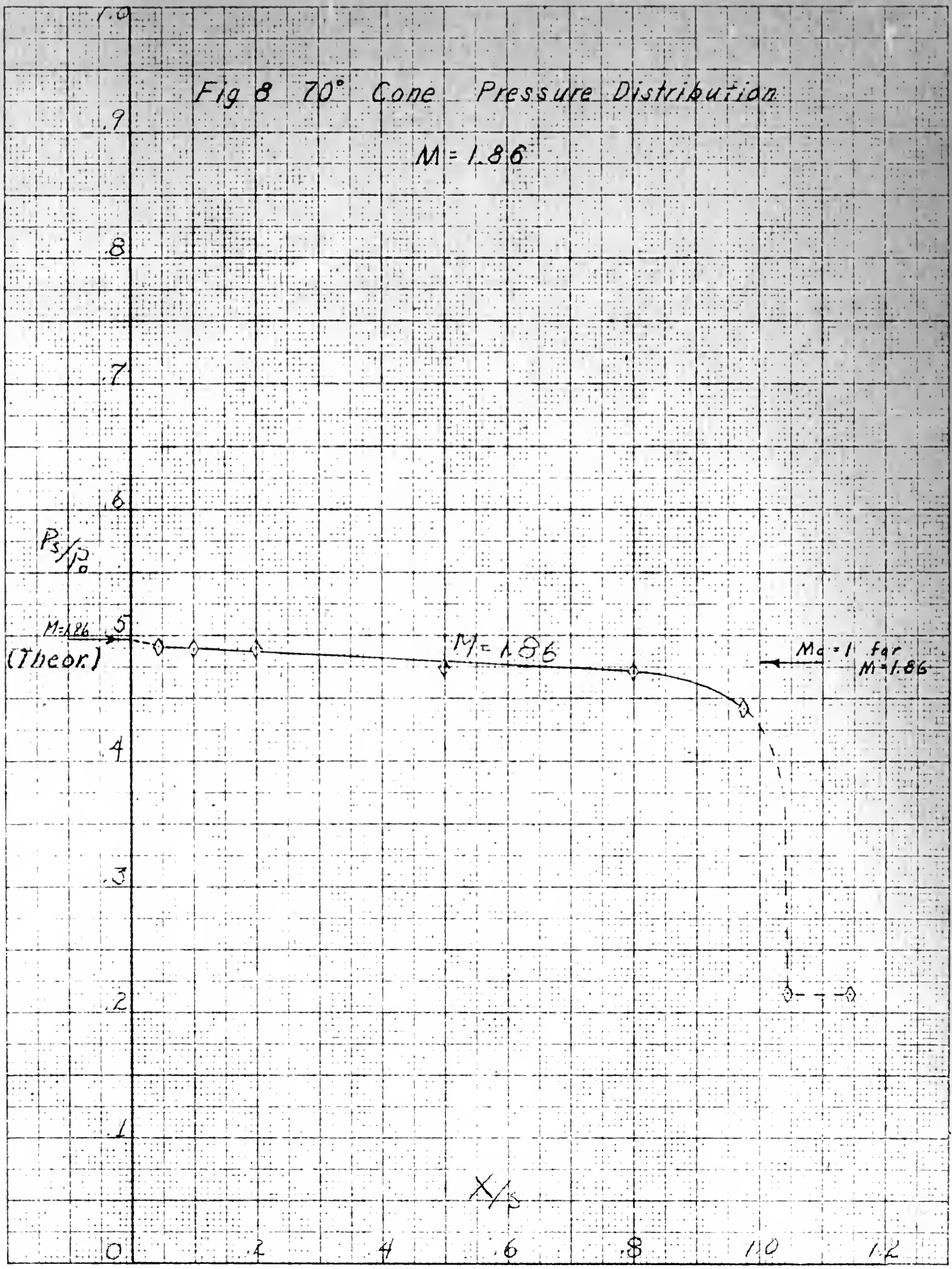
Fig 8 70° Cone Pressure Distribution
M = 1.86
1.0
.9
.8
.7
.6
P_s/P_o
.5
M=1.86
(Theor.)
M = 1.86
Mc = 1 for
M = 1.86
.4
.3
.2
.1
0
X/r
.2
.4
.6
.8
1.0
1.2

Fig 9 70° Cone Pressure Distribution

M = 1.997

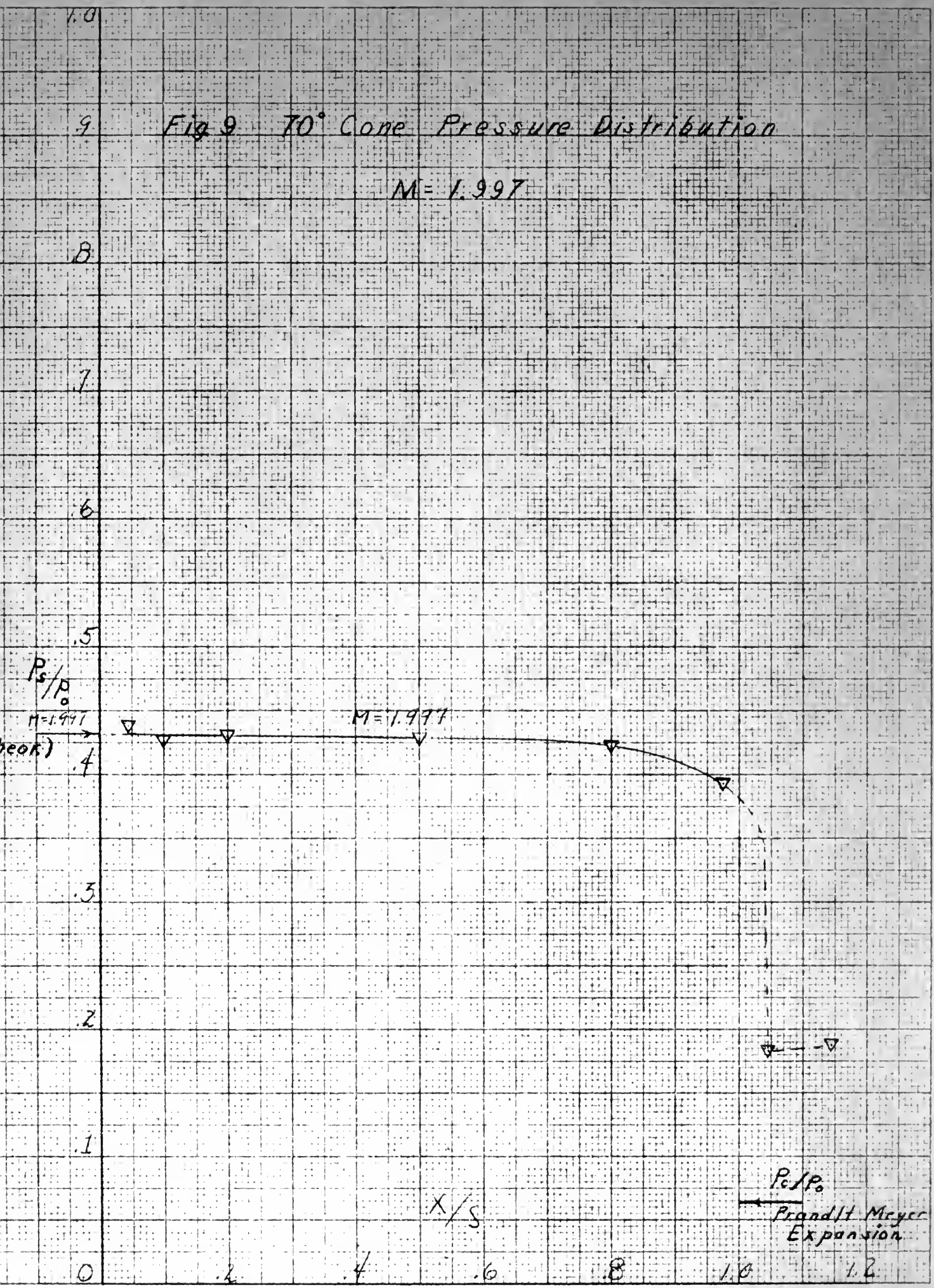

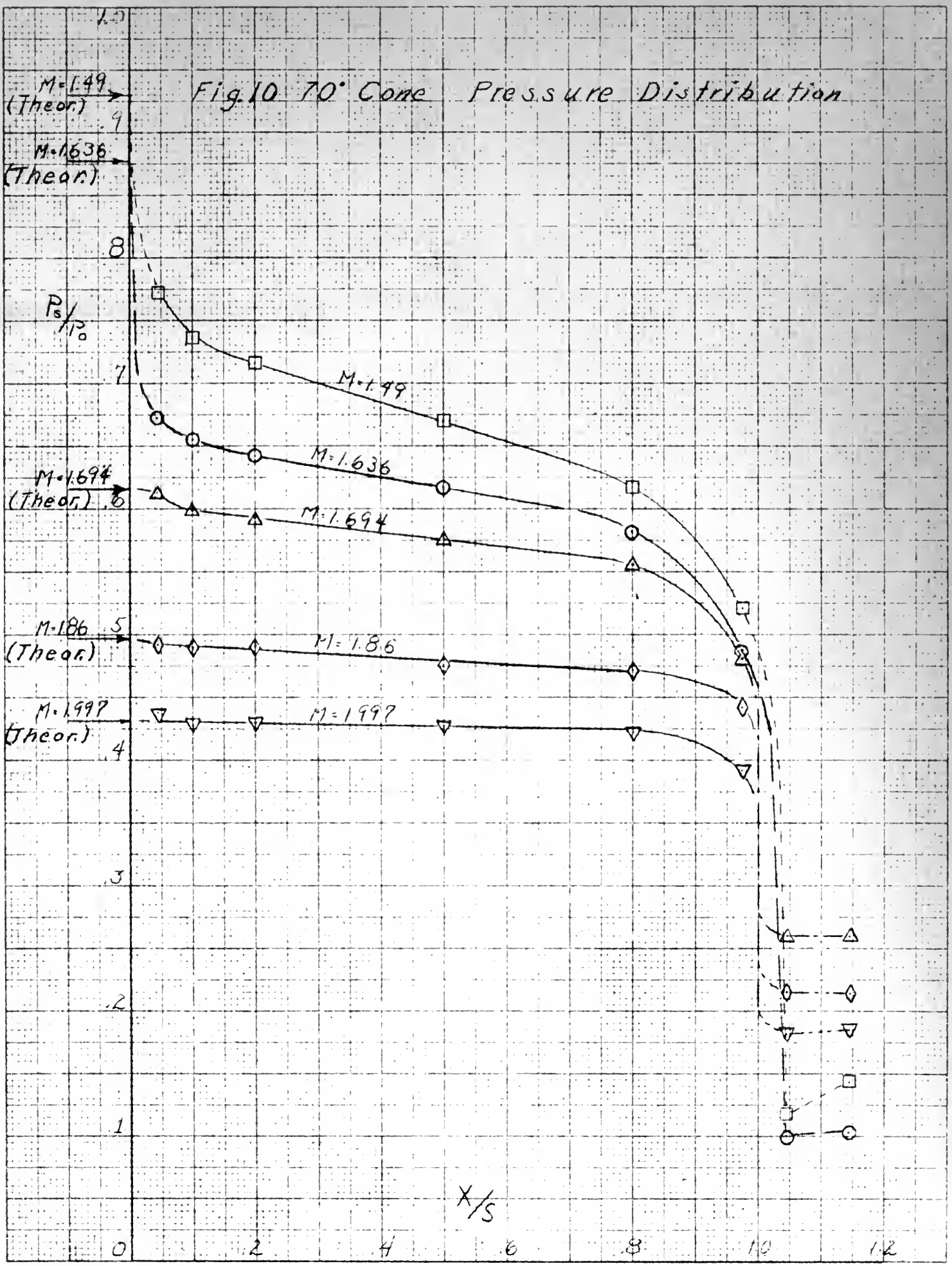
Fig. 10 70° Cone Pressure Distribution
M=1.99 (Theor.)
M=1.636 (Theor.)
M=1.694 (Theor.)
M=1.86 (Theor.)
M=1.997 (Theor.)
M=1.99
M=1.636
M=1.694
M=1.86
M=1.997
Ps/P0
X/S
1.0
.9
.8
.7
.6
.5
.4
.3
.2
.1
0
2
4
6
8
10
12

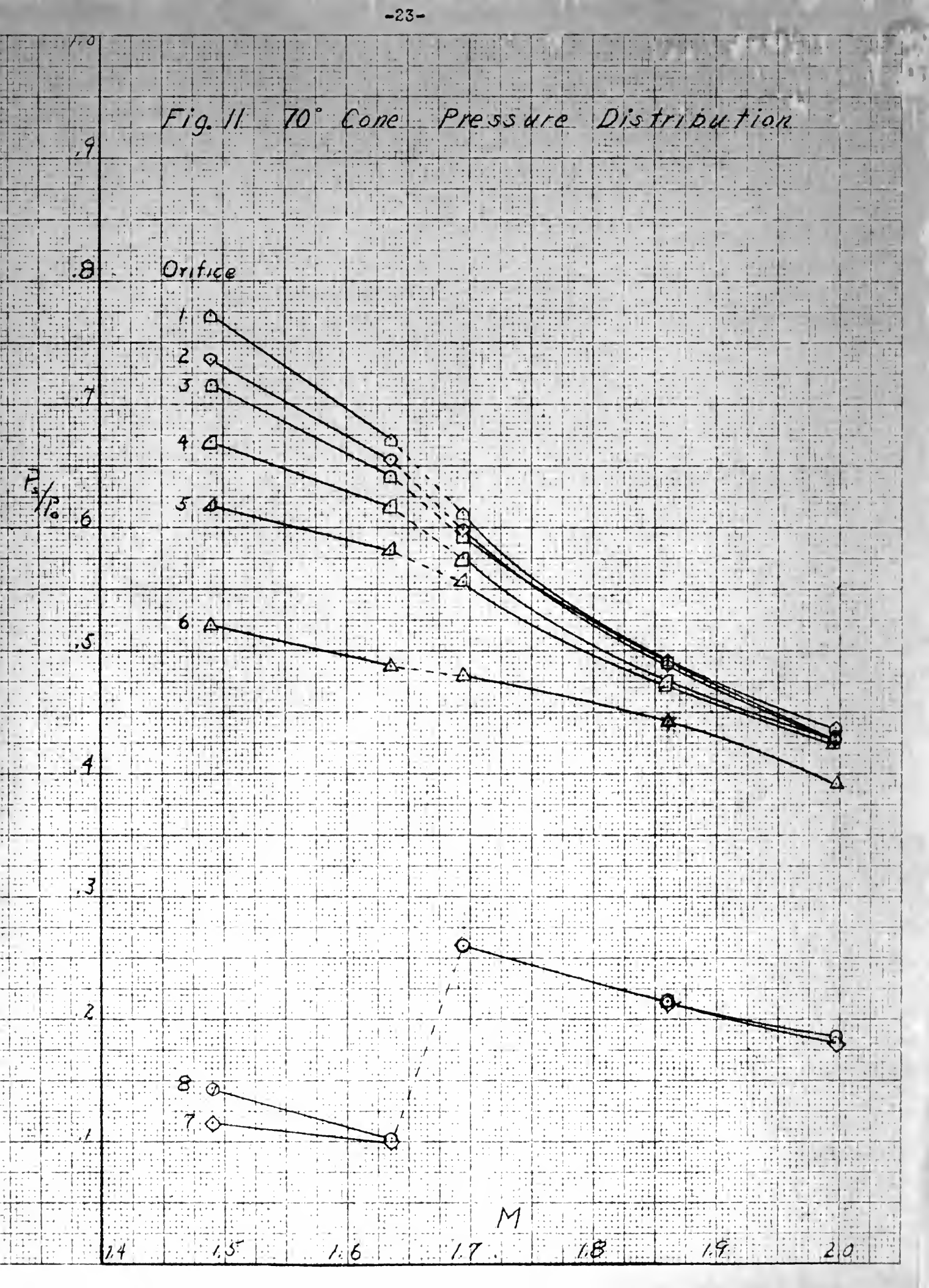
Fig. 11 70° Cone Pressure Distribution
Orifice
1
2
3
4
5
6
7
8
P_s/P_o
1.0
.9
.8
.7
.6
.5
.4
.3
.2
.1
M
1.4
1.5
1.6
1.7
1.8
1.9
2.0

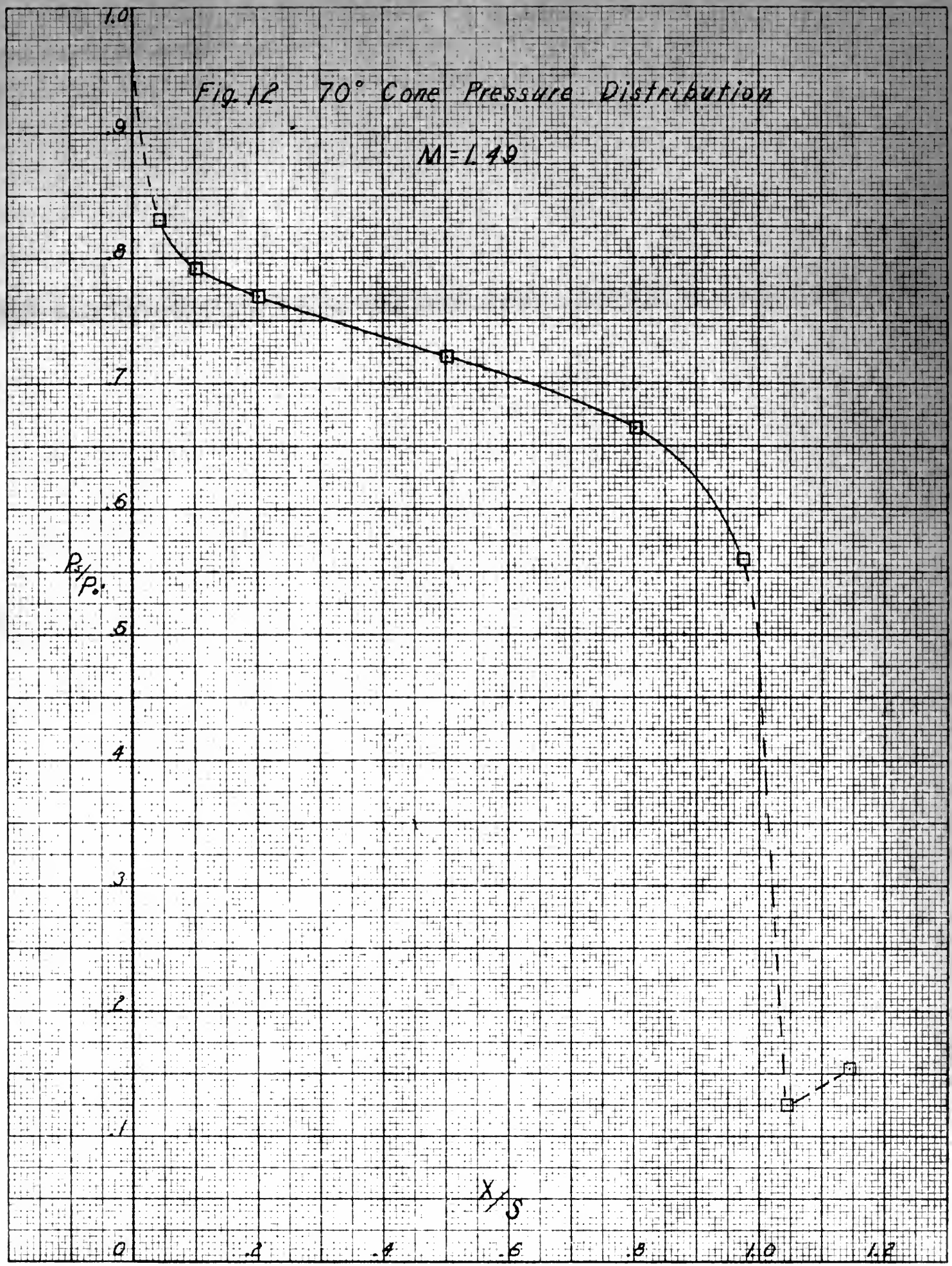
Fig. 12 70° Cone Pressure Distribution
M = 1.49
1.0
.9
.8
.7
.6
P_s/P_o
.5
.4
.3
.2
.1
0
X/S
.2
.4
.6
.8
1.0
1.2

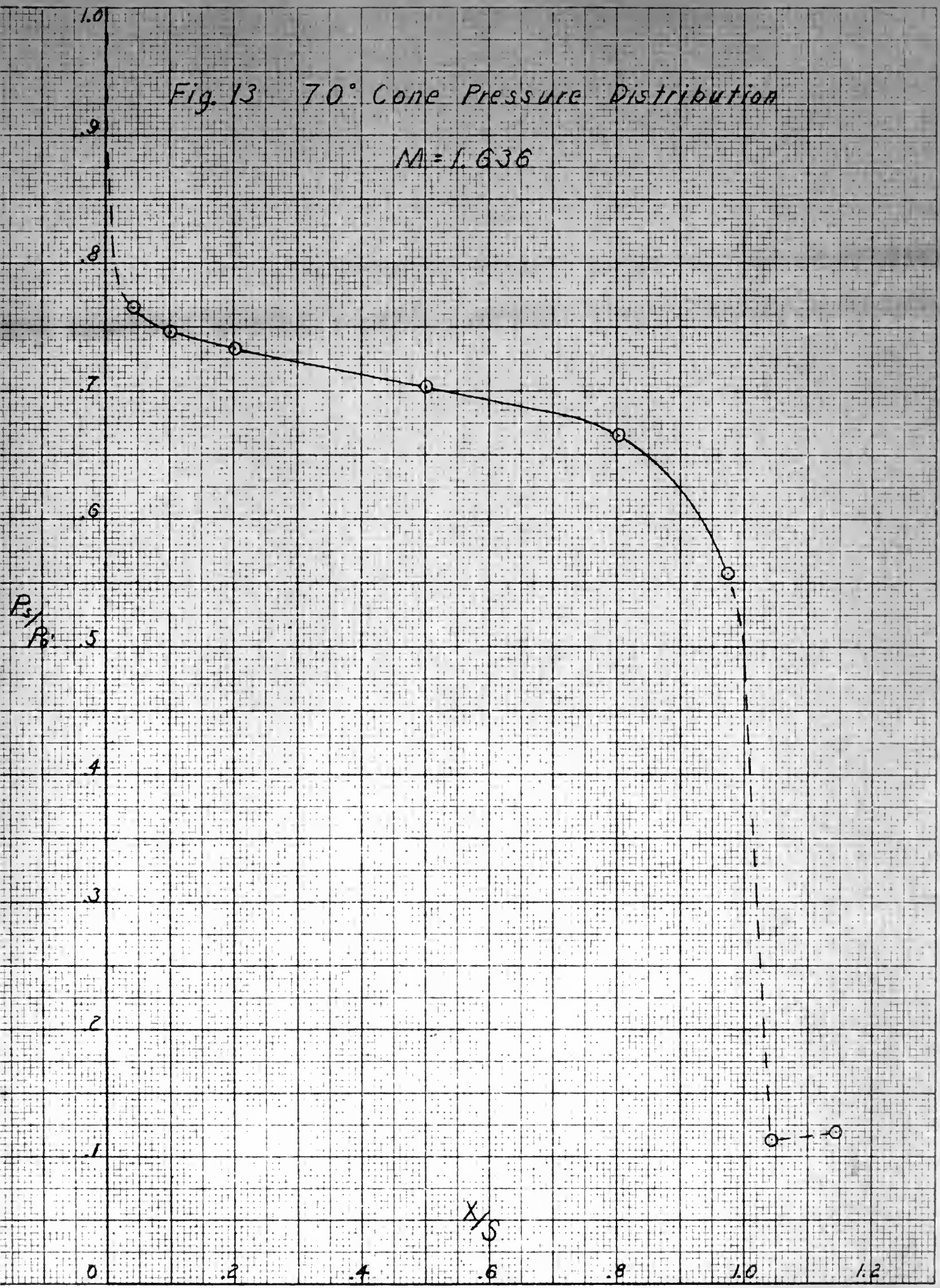
Fig. 13 70° Cone Pressure Distribution
M = 1.636
1.0
.9
.8
.7
.6
P_s/P_0
.5
.4
.3
.2
.1
0
X/S
.2
.4
.6
.8
1.0
1.2

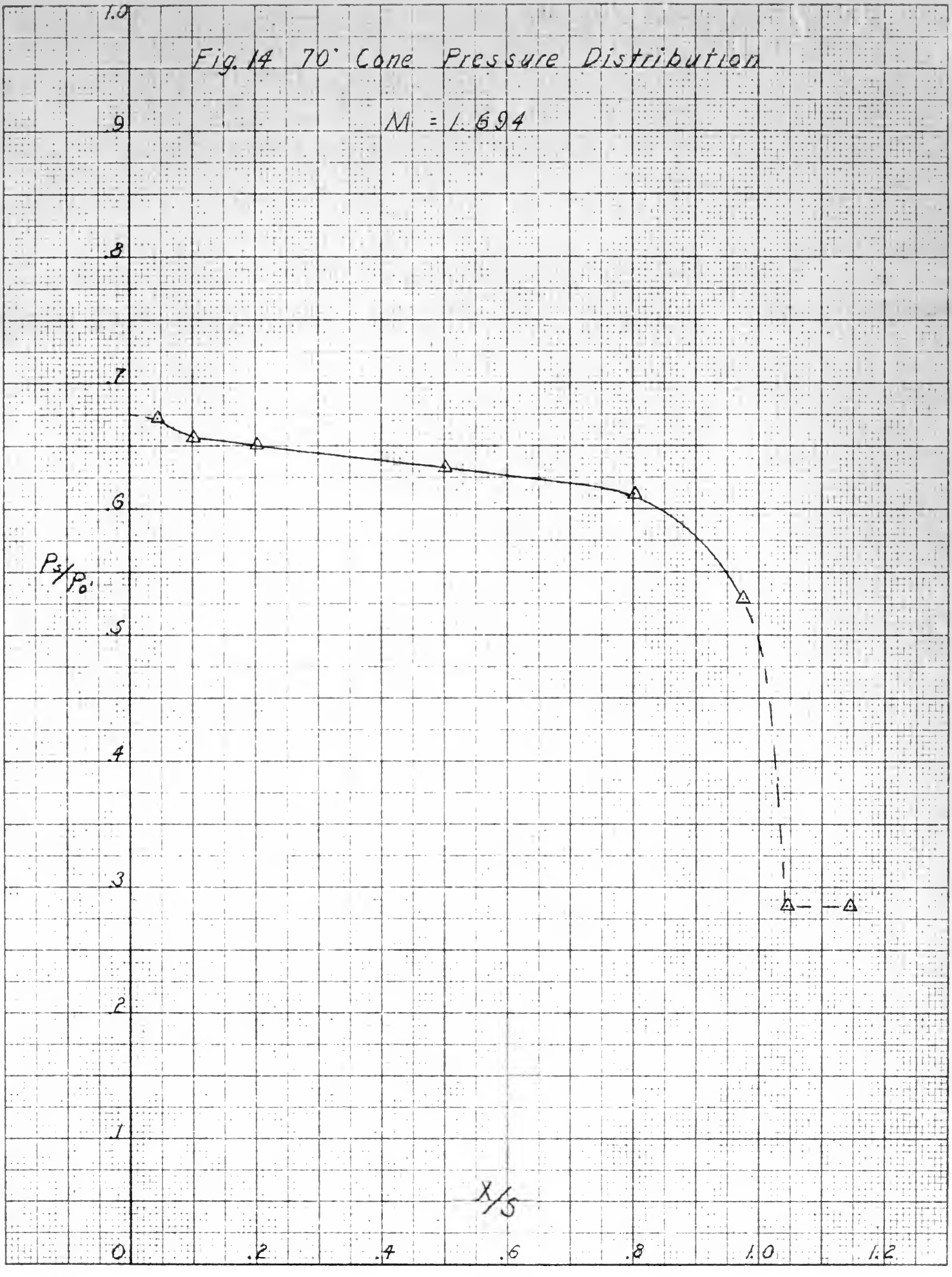
Fig. 14 70° Cone Pressure Distribution
M = 1.694
1.0
.9
.8
.7
.6
P_s/P_o
.5
.4
.3
.2
.1
0
X/S
.2
.4
.6
.8
1.0
1.2

Fig. 15 70° Cone Pressure Distribution

M = 1.86

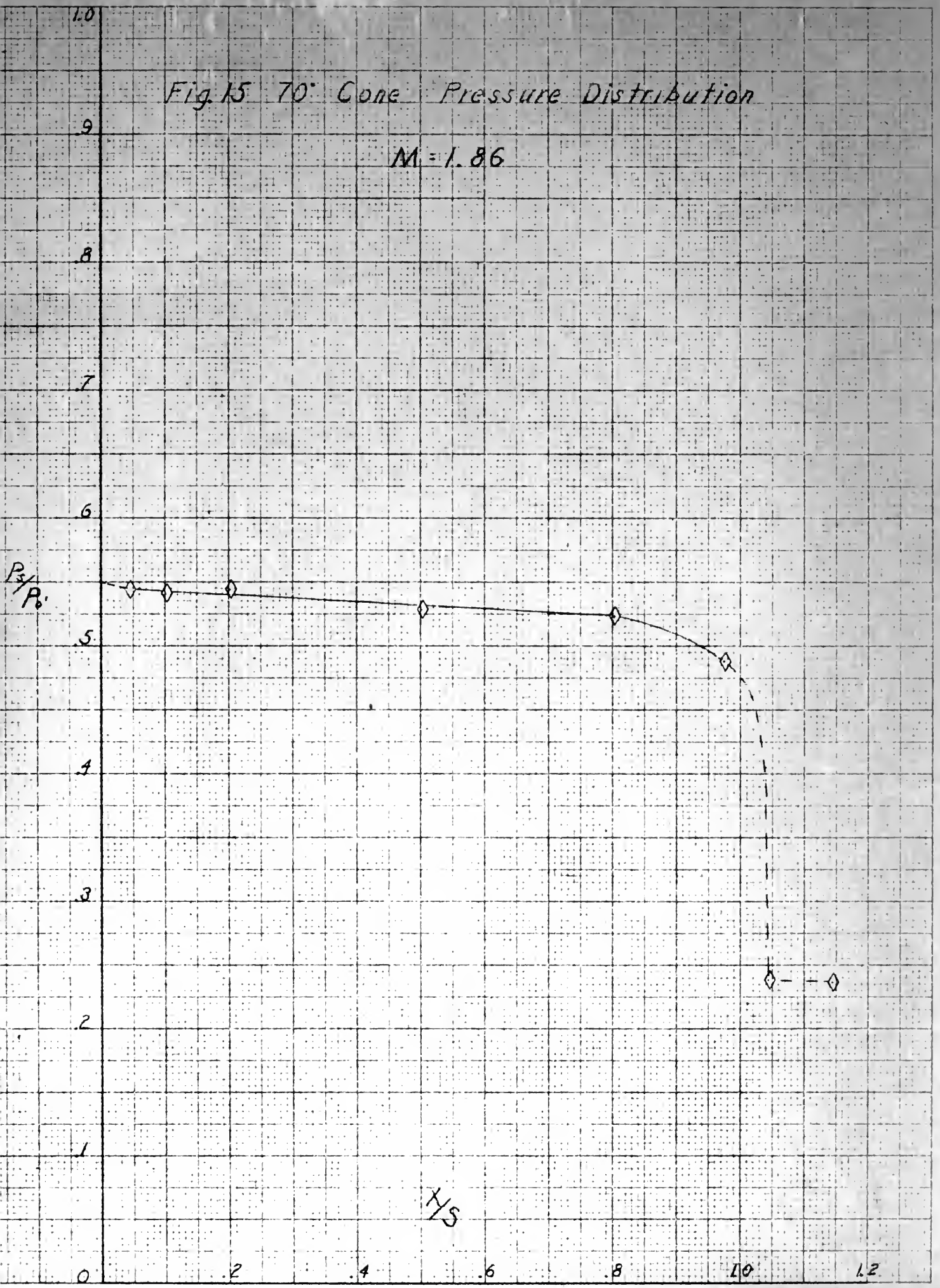

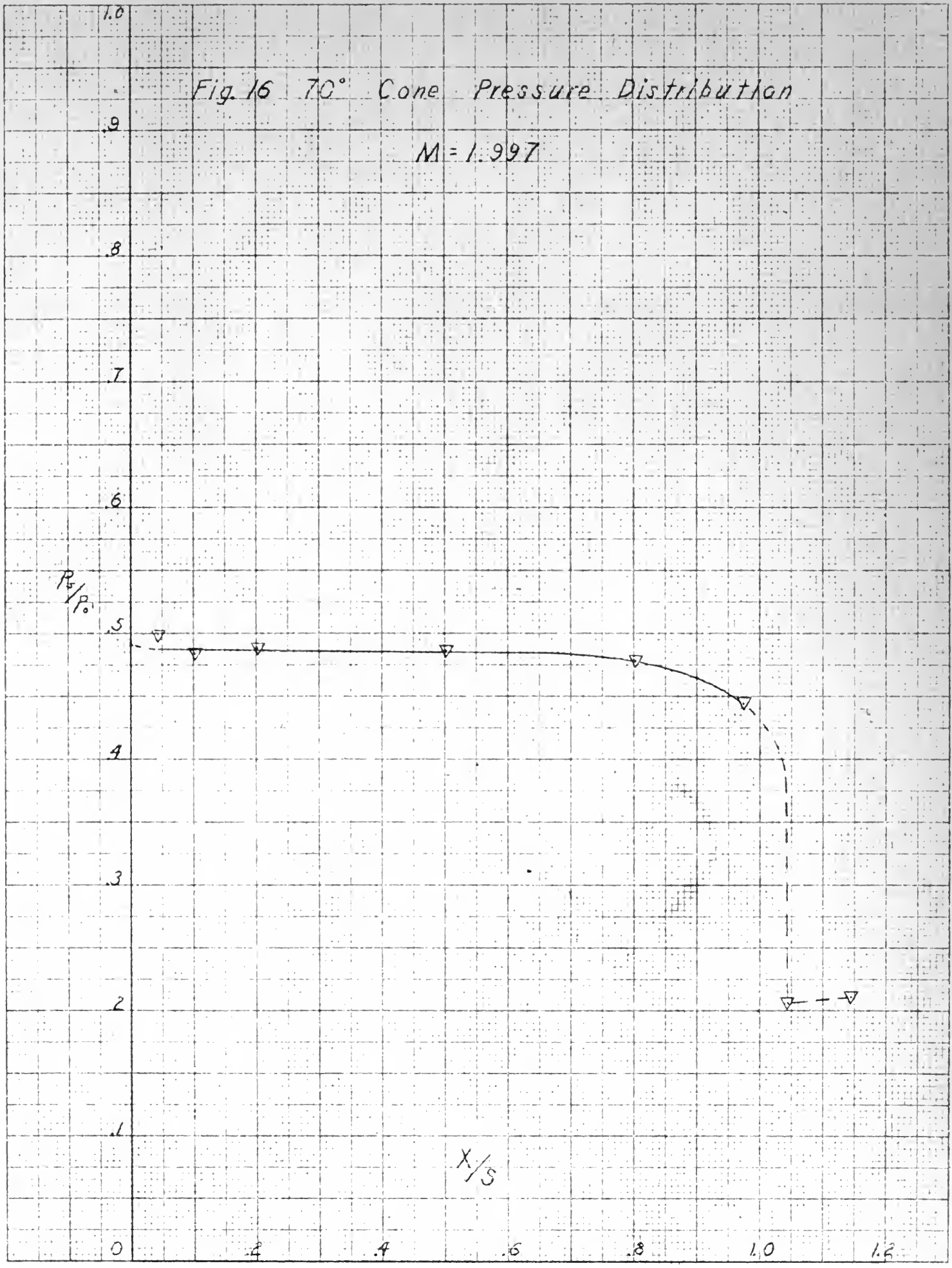
Fig. 16 70° Cone Pressure Distribution
M = 1.997
1.0
.9
.8
.7
.6
P_s/P_o
.5
.4
.3
.2
.1
0
X/S
.2
.4
.6
.8
1.0
1.2

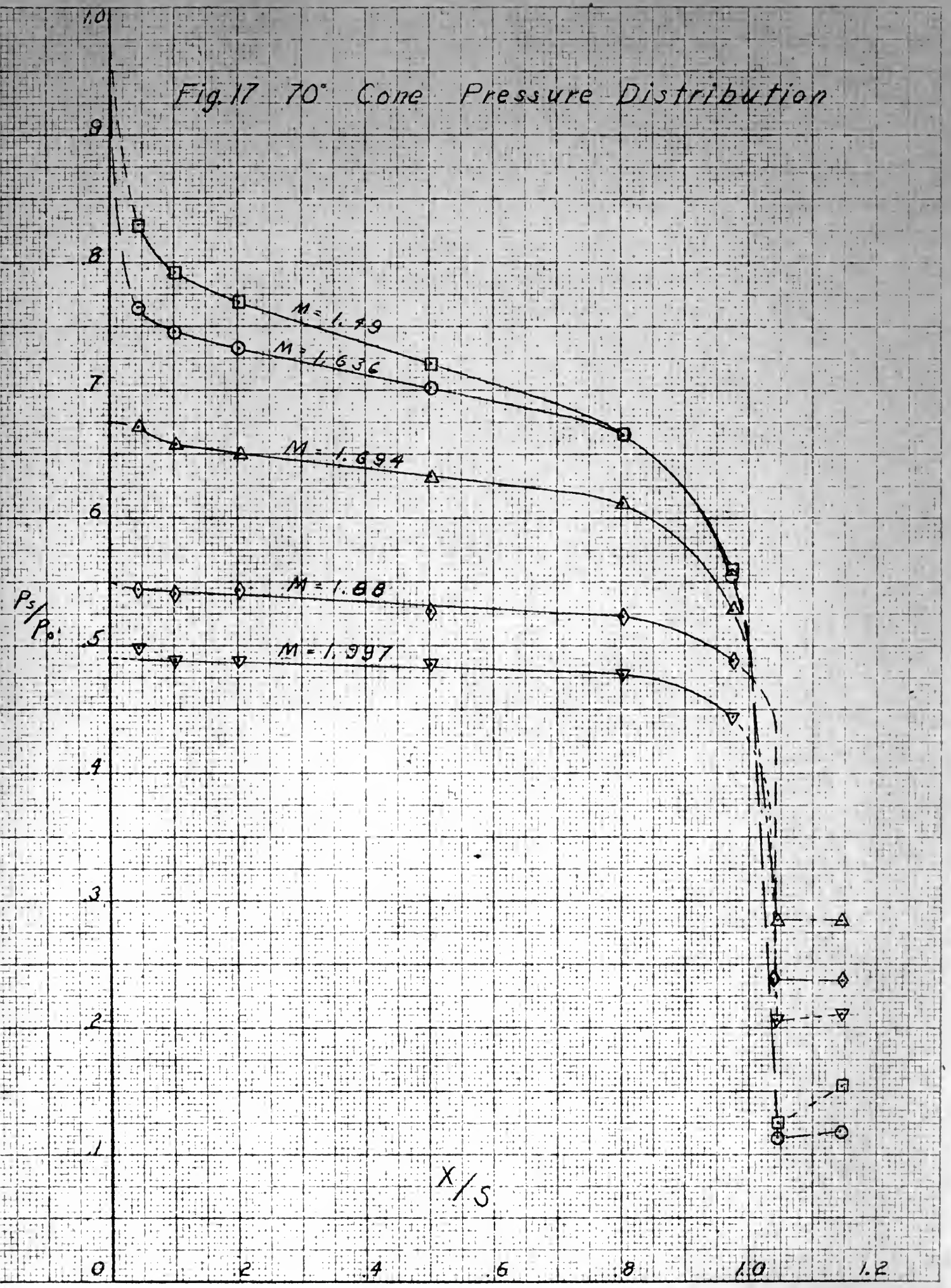
Fig. 17 70° Cone Pressure Distribution
M = 1.749
M = 1.636
M = 1.694
M = 1.888
M = 1.997
P_s/P_o
X/S
1.0
.9
.8
.7
.6
.5
.4
.3
.2
.1
0
.2
.4
.6
.8
1.0
1.2

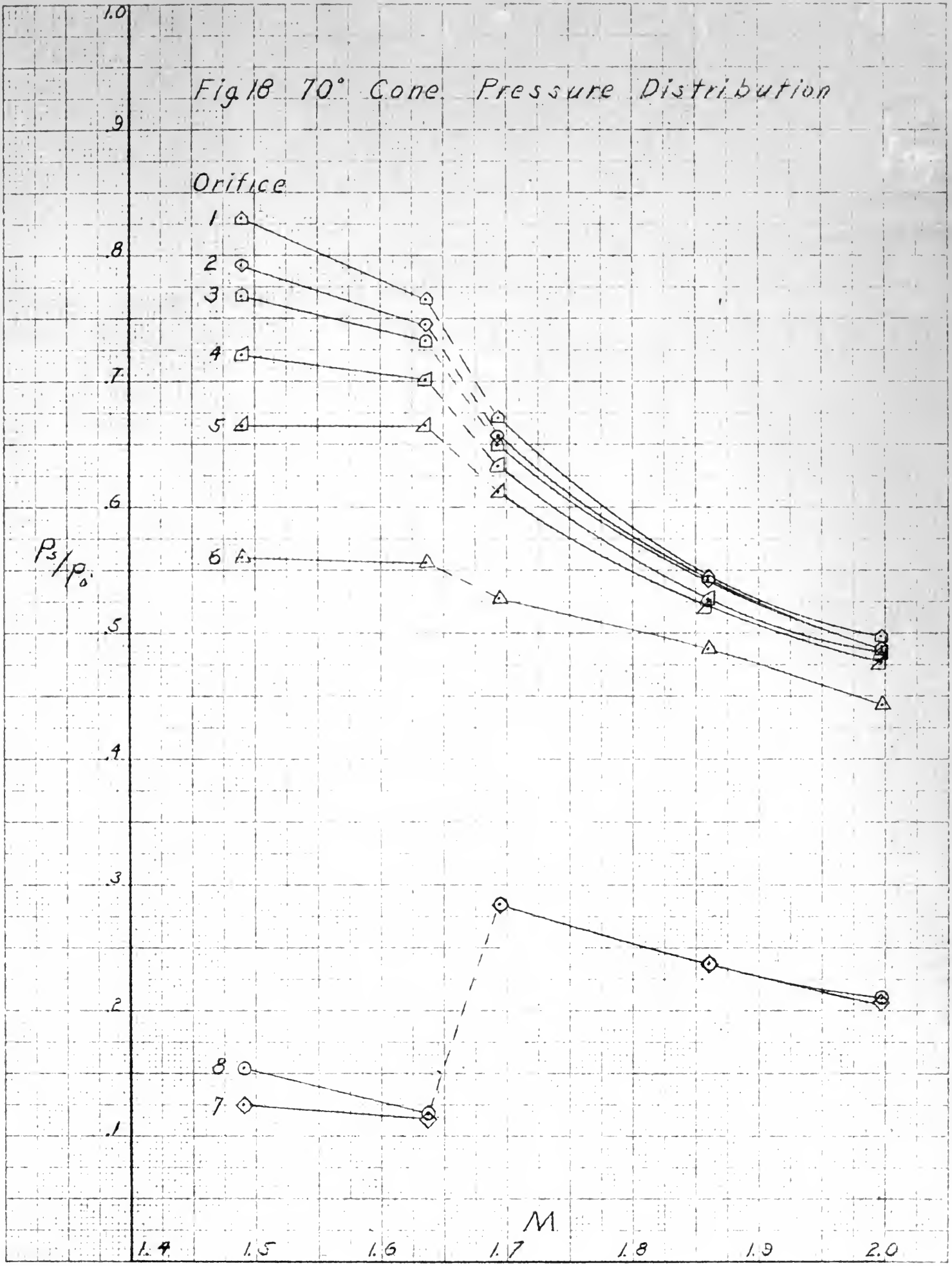
Fig 18 70° Cone Pressure Distribution
Orifice
1
2
3
4
5
6
8
7
P_3/P_0
1.0
.9
.8
.7
.6
.5
.4
.3
.2
.1
M
1.4
1.5
1.6
1.7
1.8
1.9
2.0

Fig. 19 70° Cone Shock Wave Pattern

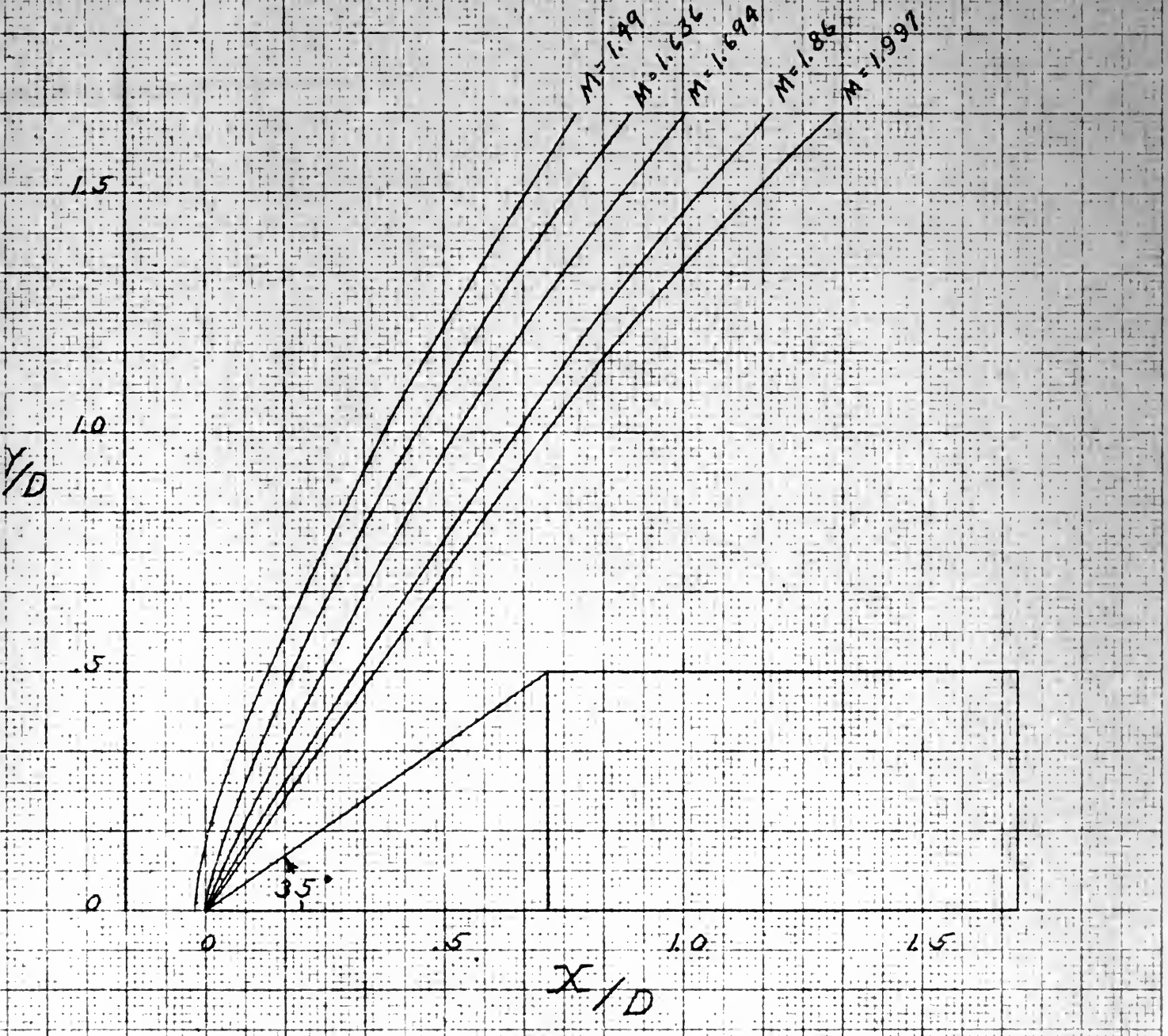

Fig 20 70° Cone Shock Wave Angle and Mach Number After Shock

M = 1.49

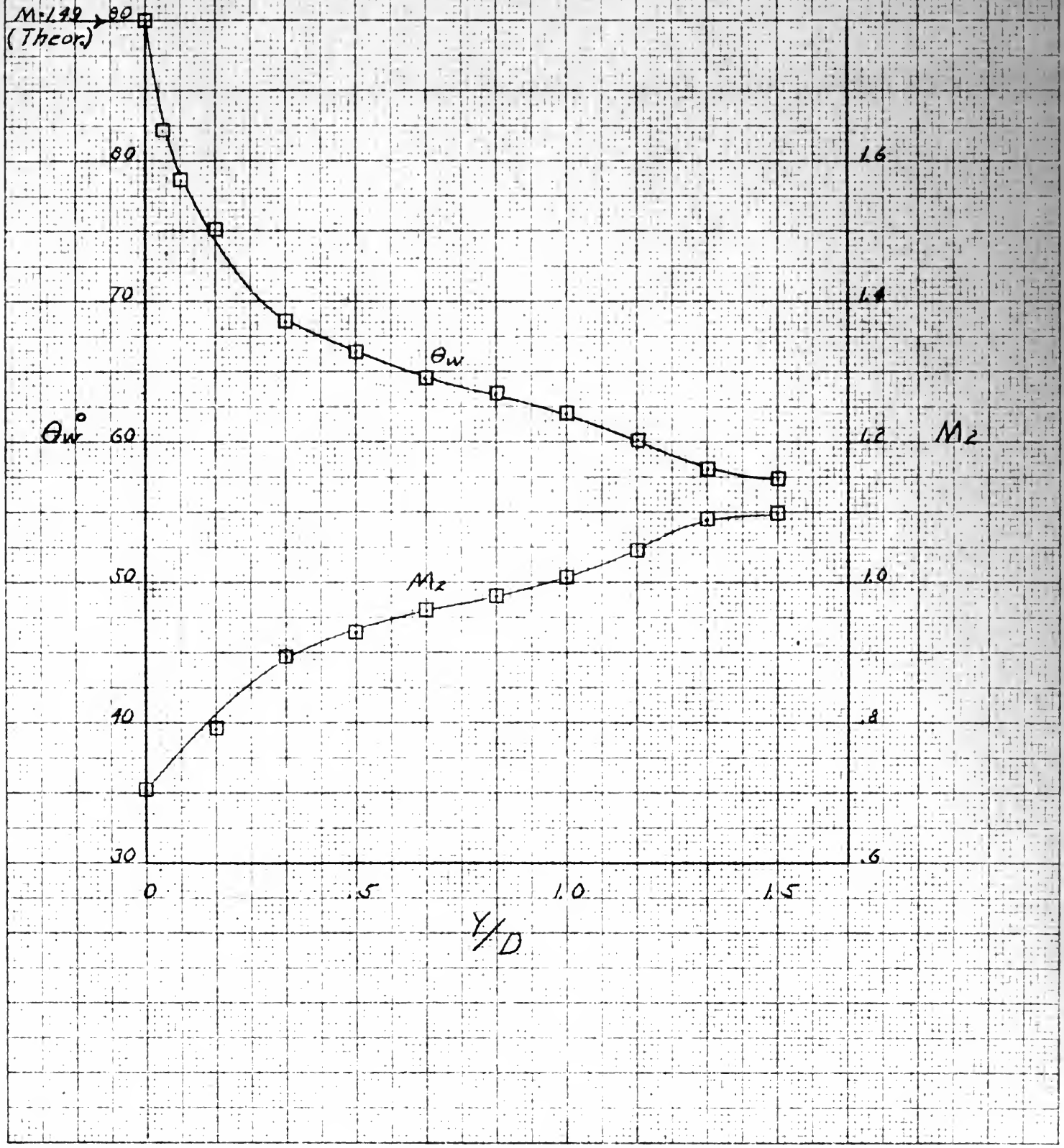

Fig. 22 70° Cone Shock Wave Angle and Mach Number After Shock

M = 1.694

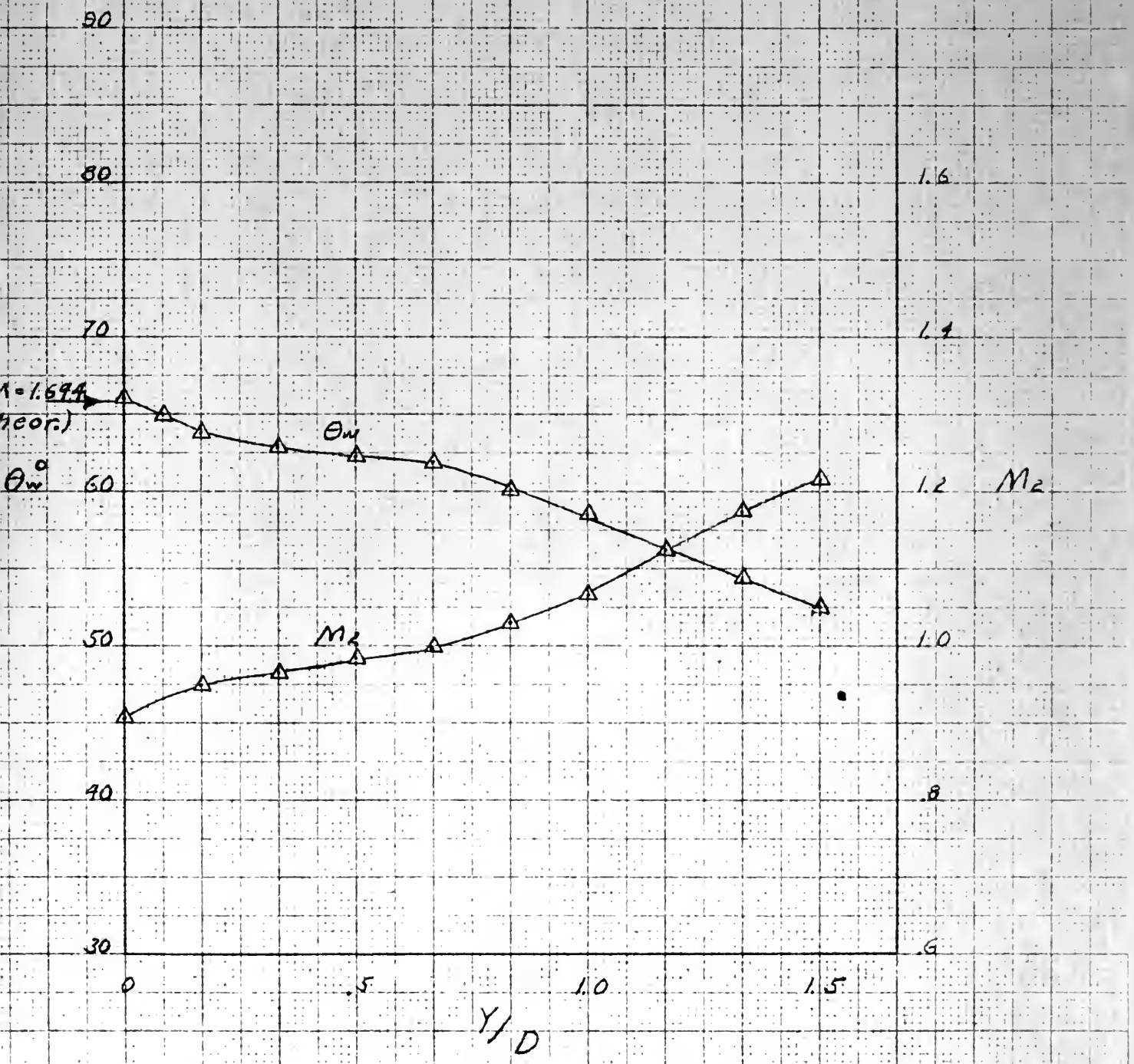

Fig. 21 20° Cone Shock Wave Angle and Mach Number After Shock

M = 1.636

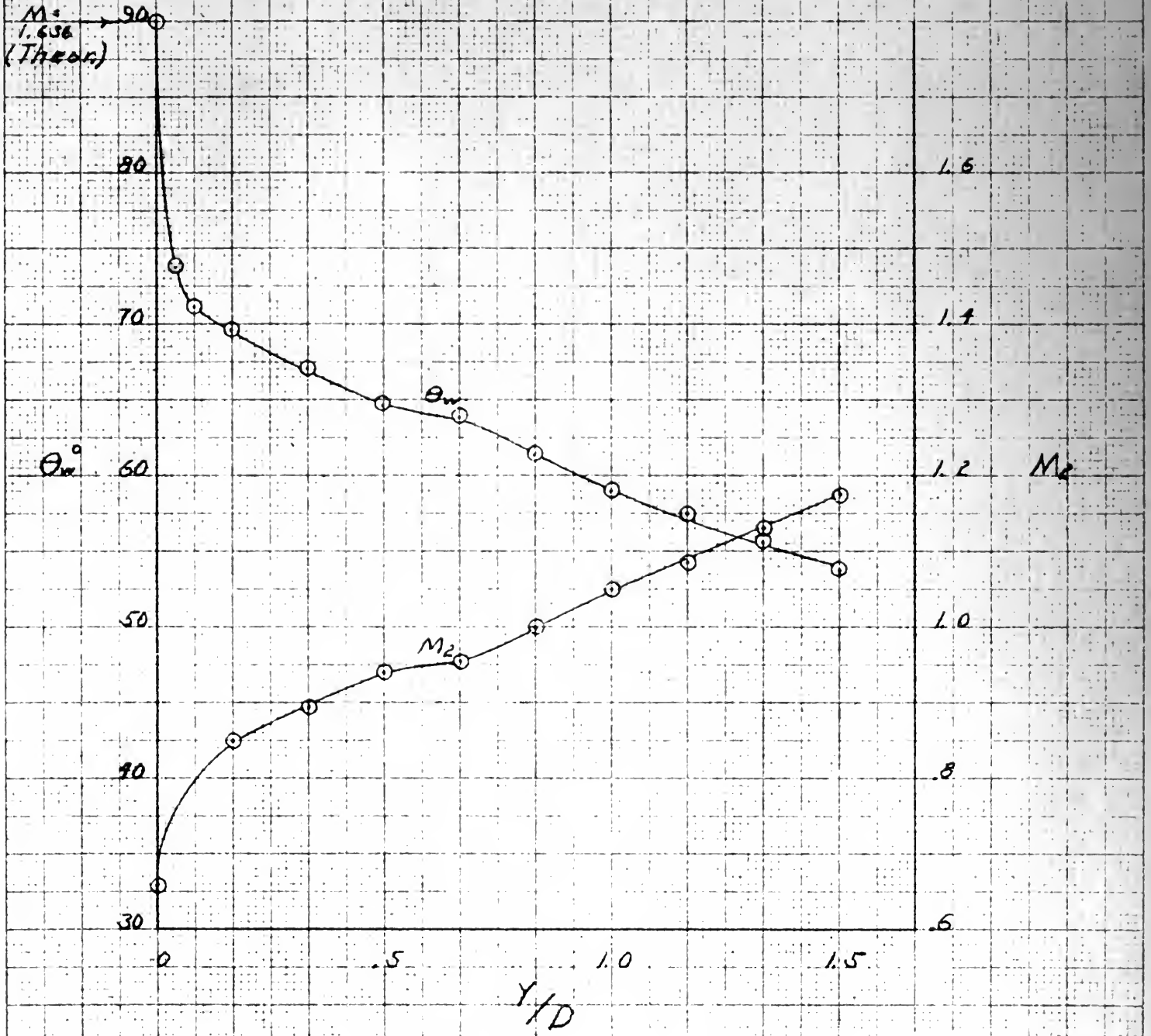

Fig 23 70° Cone Shock Wave Angle and Mach Number After Shock

M = 1.86

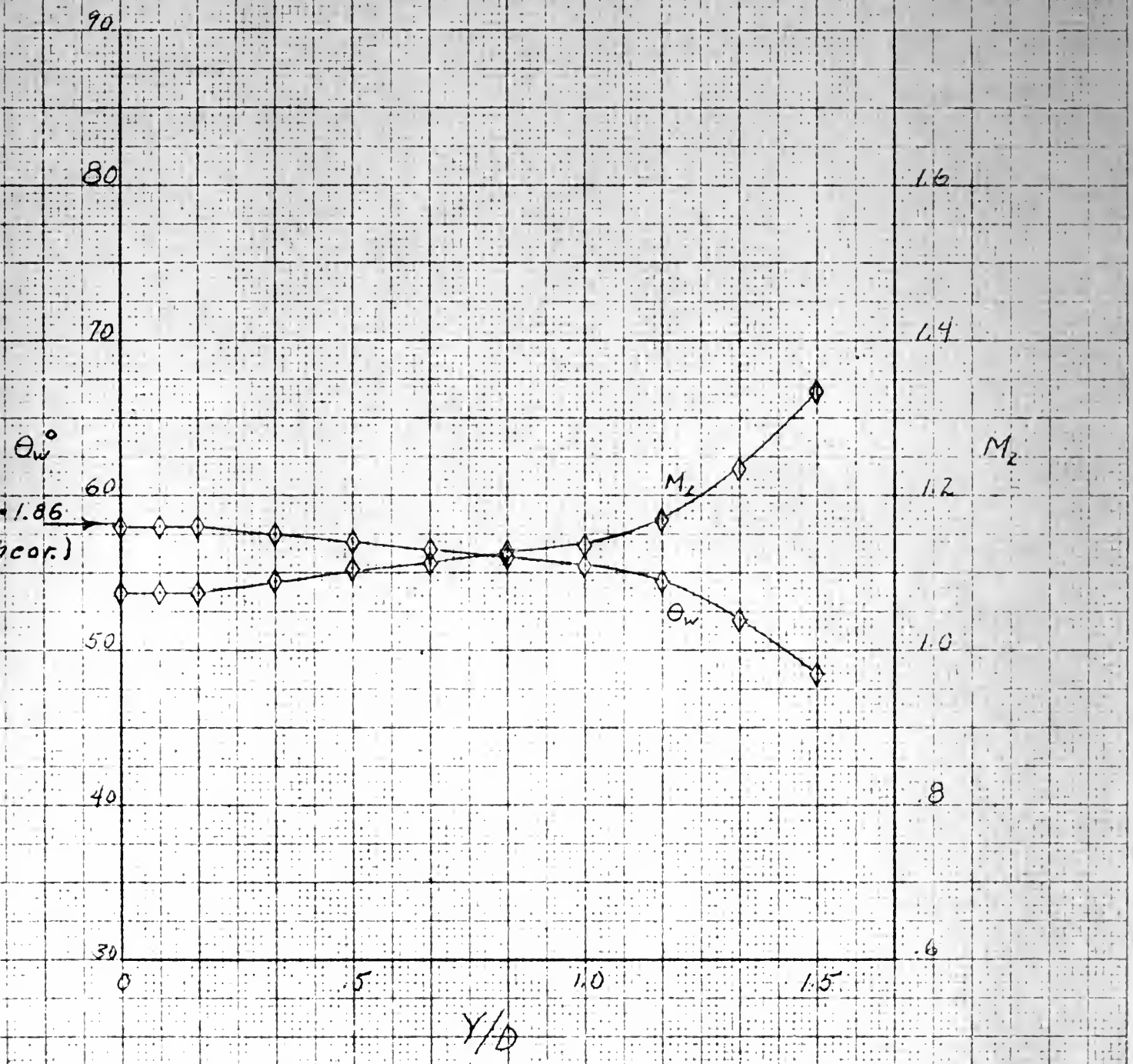

Fig. 24 70° Cone Shock Wave Angle and Mach Number After Shock
M = 1.997

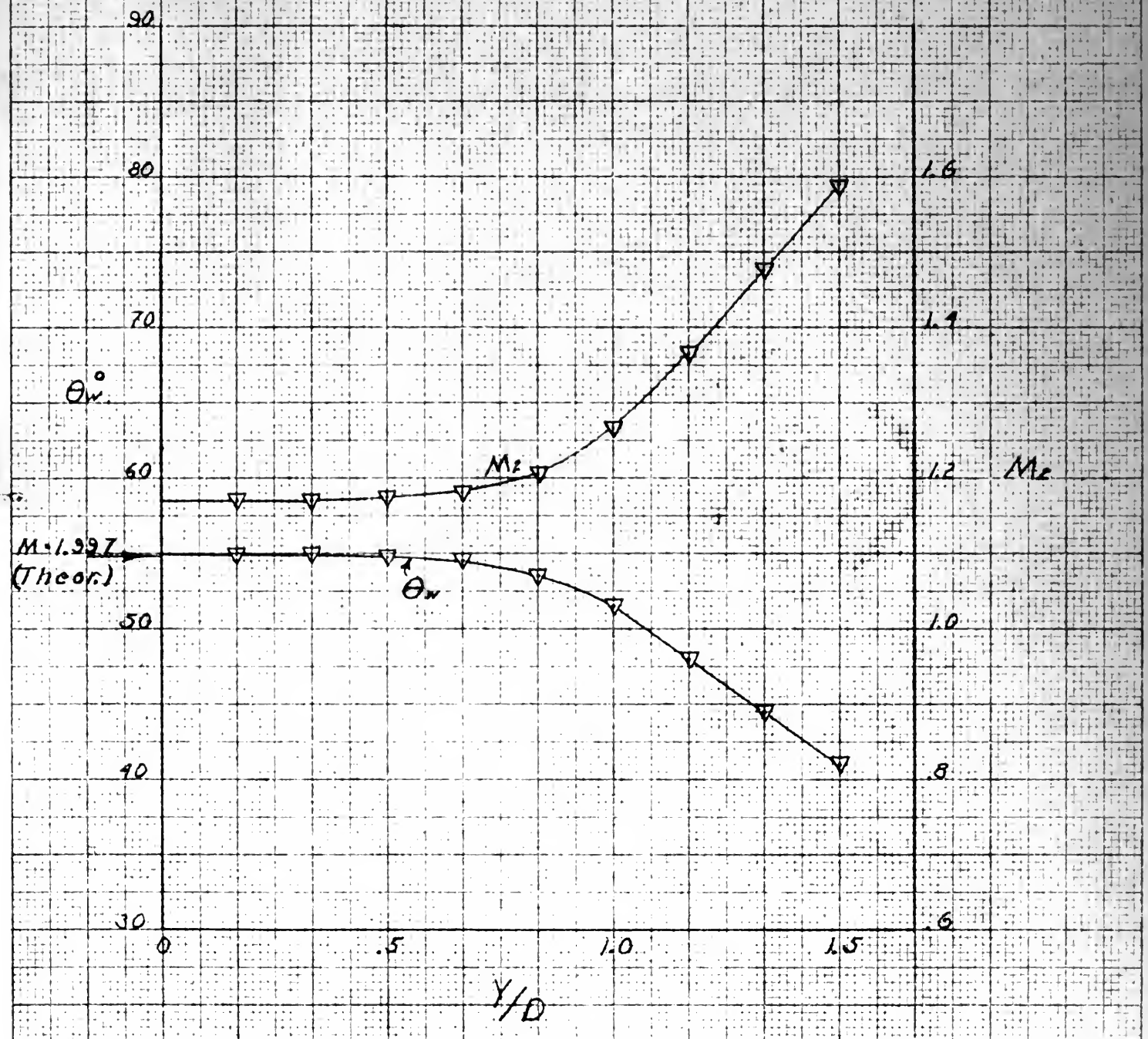

Fig. 25 70° Cone Shock Wave Angle

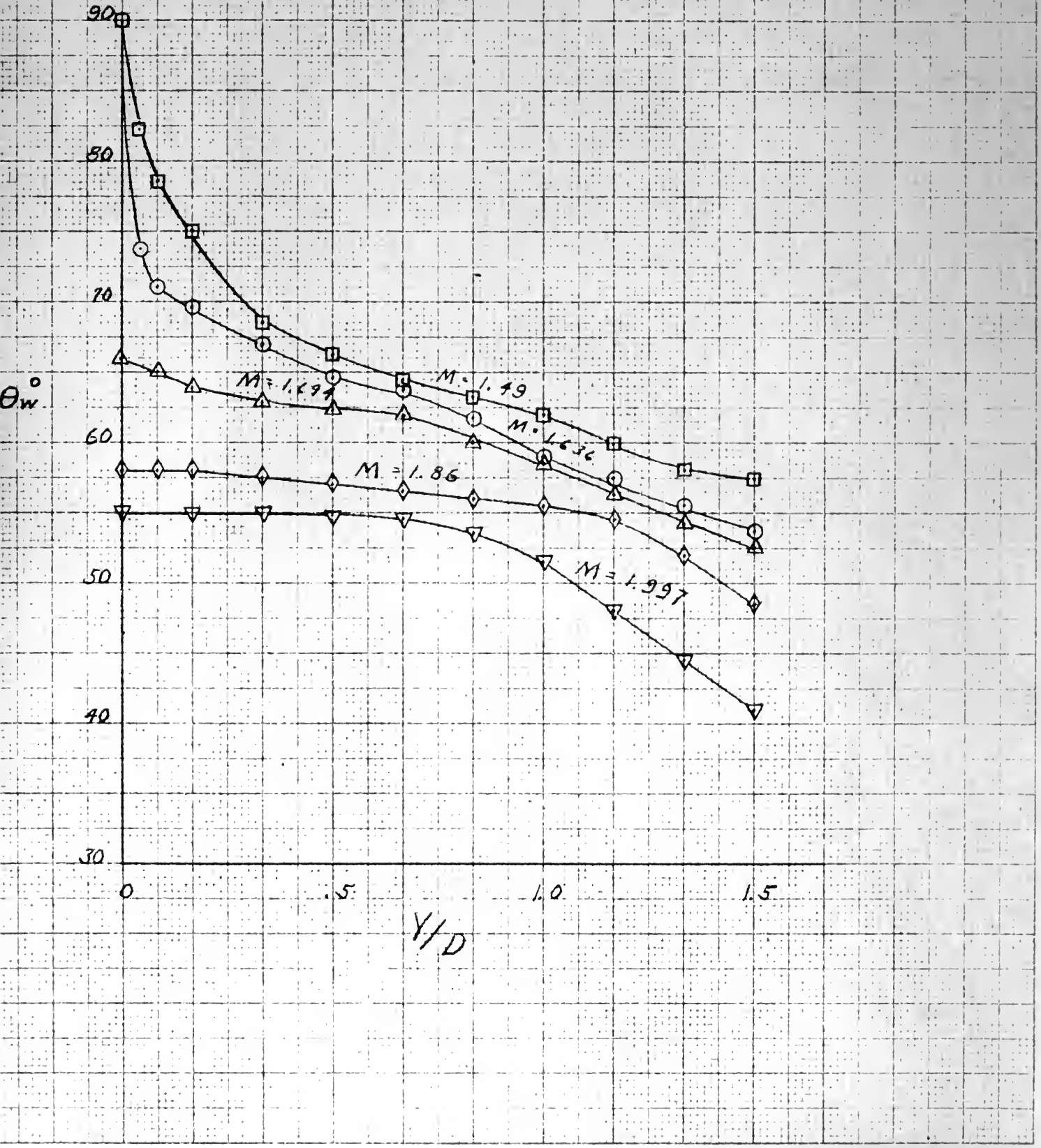

Fig. 26 70° Cone Mach Number Behind Shock

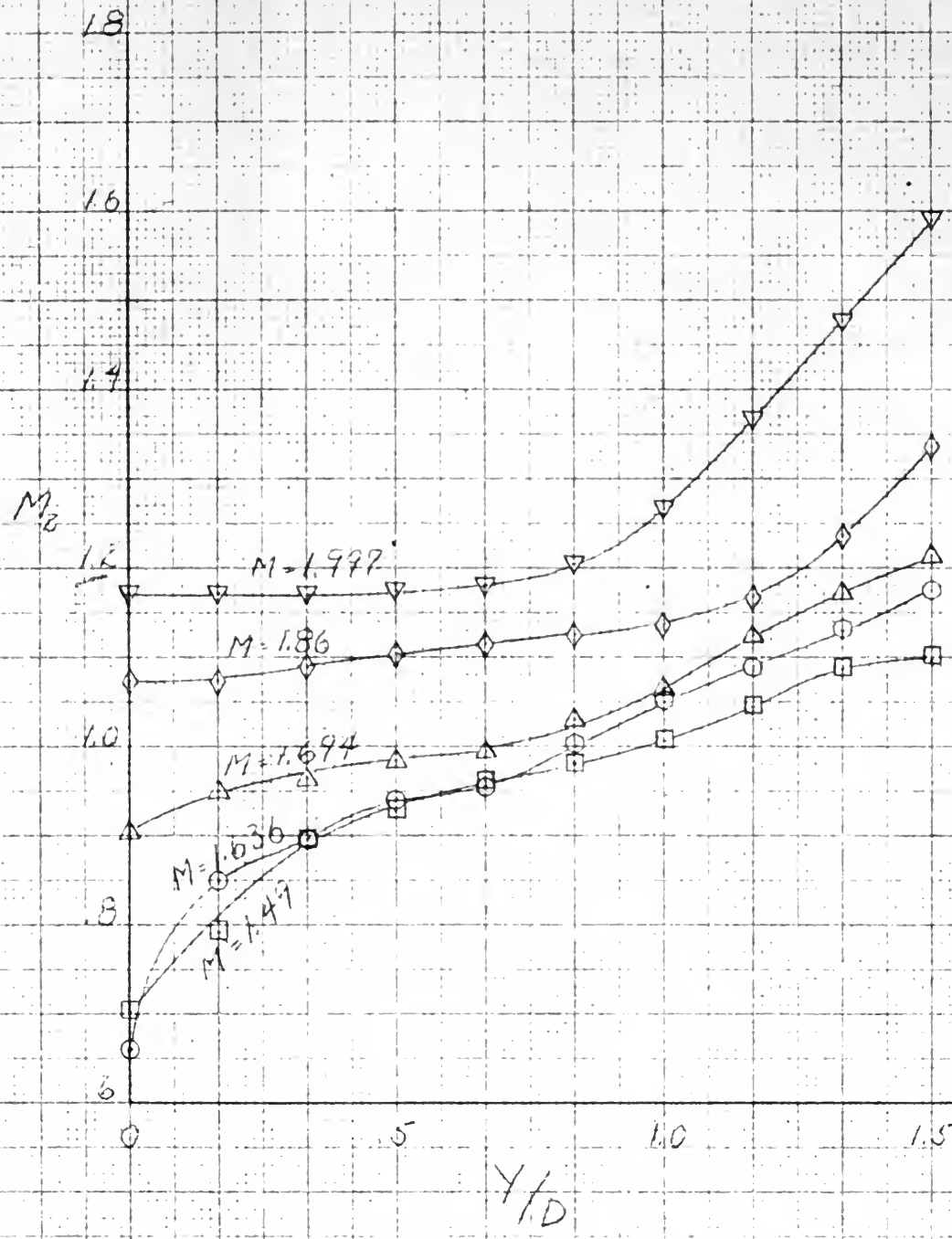

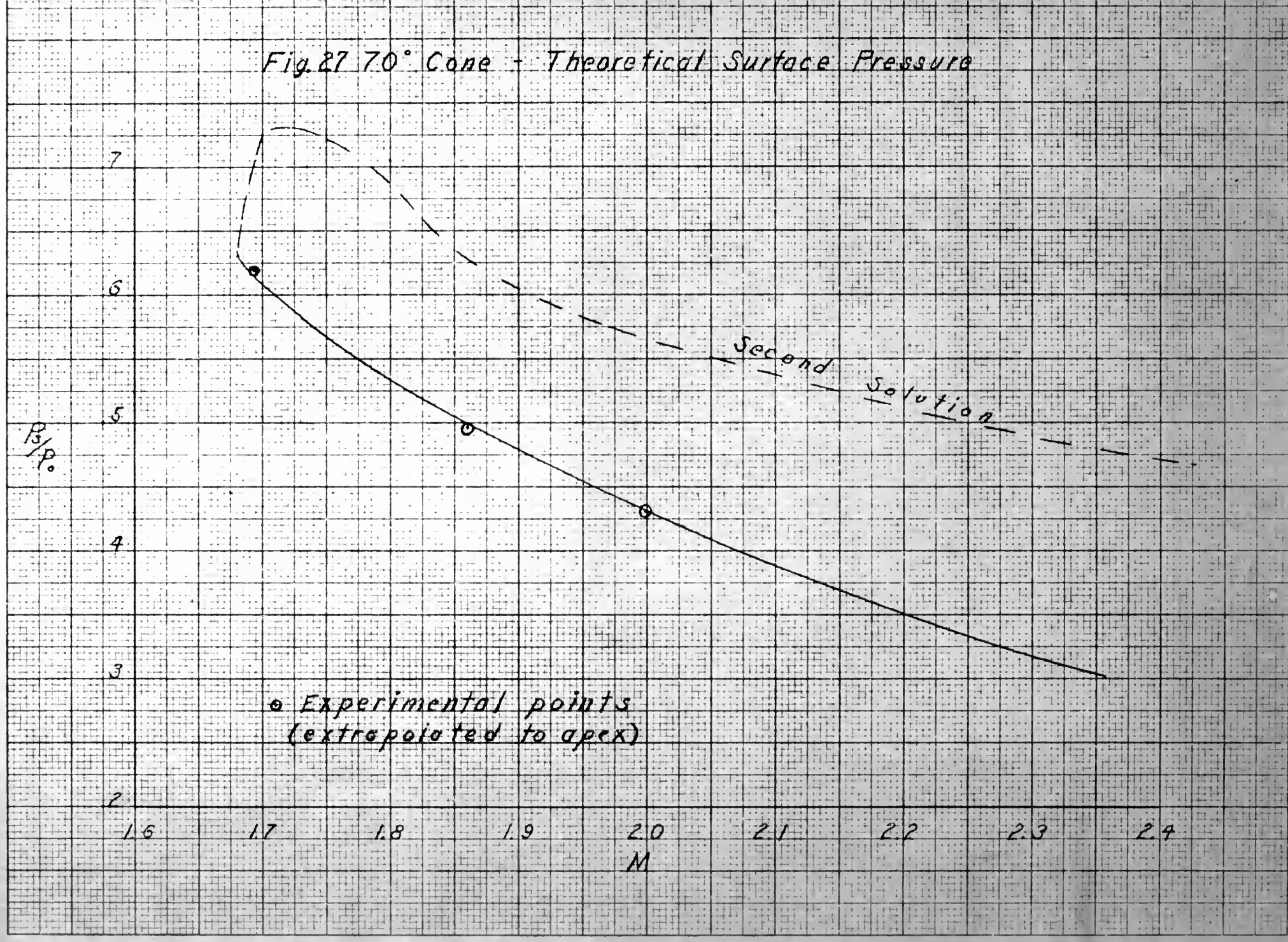
Fig. 27 70° Cone - Theoretical Surface Pressure
7
6
5
4
3
2
p_s/p_∞
Second Solution
o Experimental points
(extrapolated to apex)
1.6
1.7
1.8
1.9
2.0
2.1
2.2
2.3
2.4
M

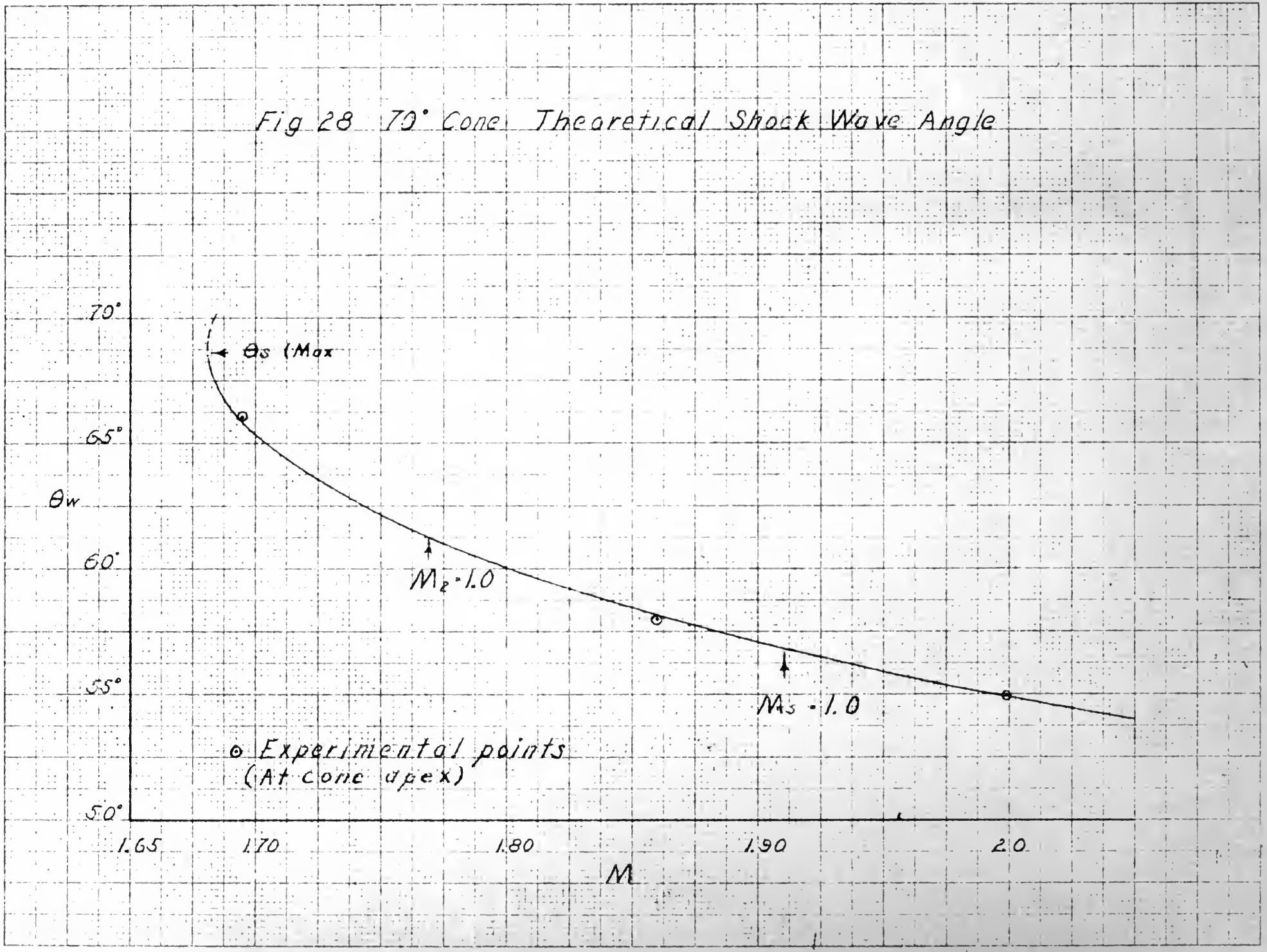
Fig 28 70° Cone Theoretical Shock Wave Angle
70°
65°
60°
55°
50°
θw
θs (Max
M2 - 1.0
M3 - 1.0
⊙ Experimental points
(At cone apex)
1.65
1.70
1.80
1.90
2.0
M

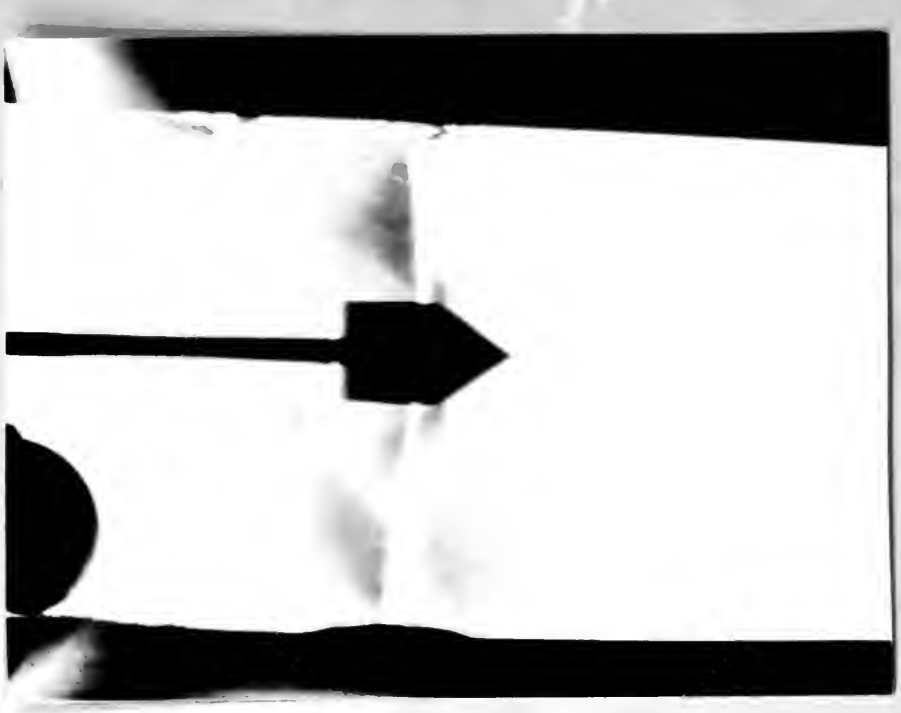

Fig. 29a

M = 1.49

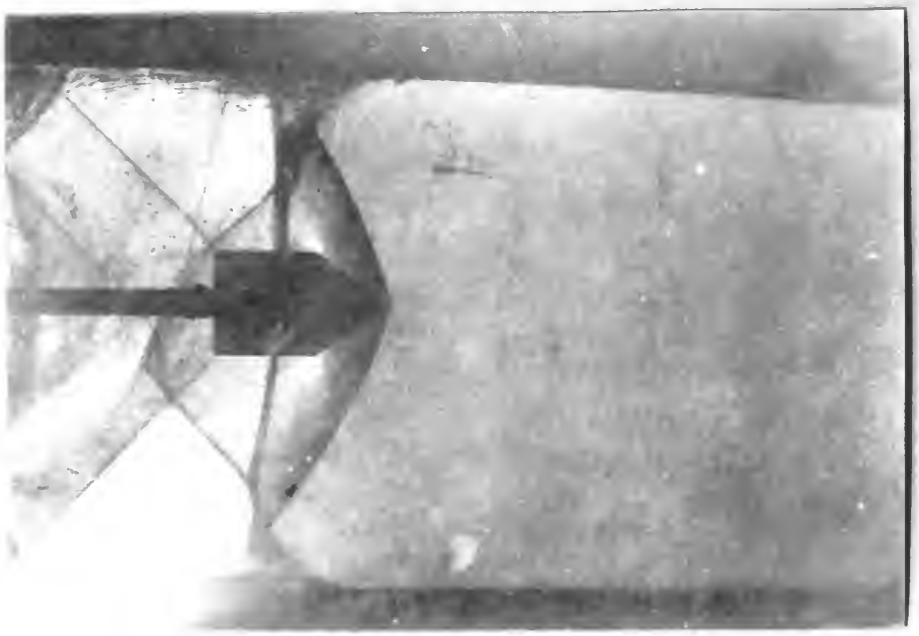

Fig. 29b

M = 1.49

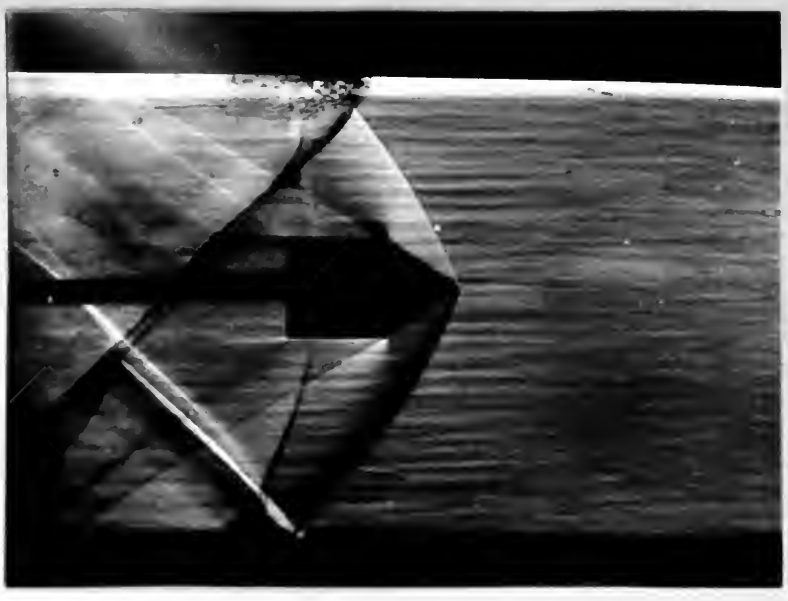

Fig. 30a

M = 1.636

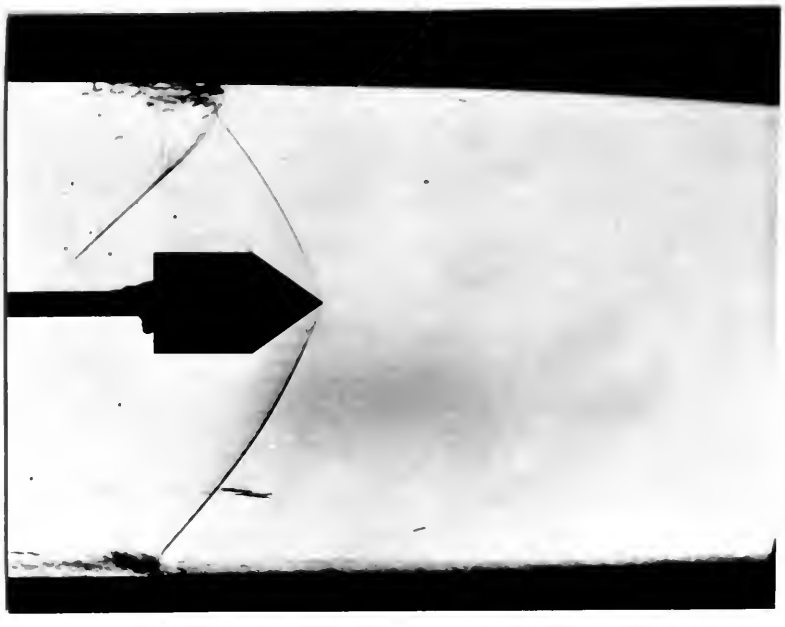

Fig. 30b

M = 1.636

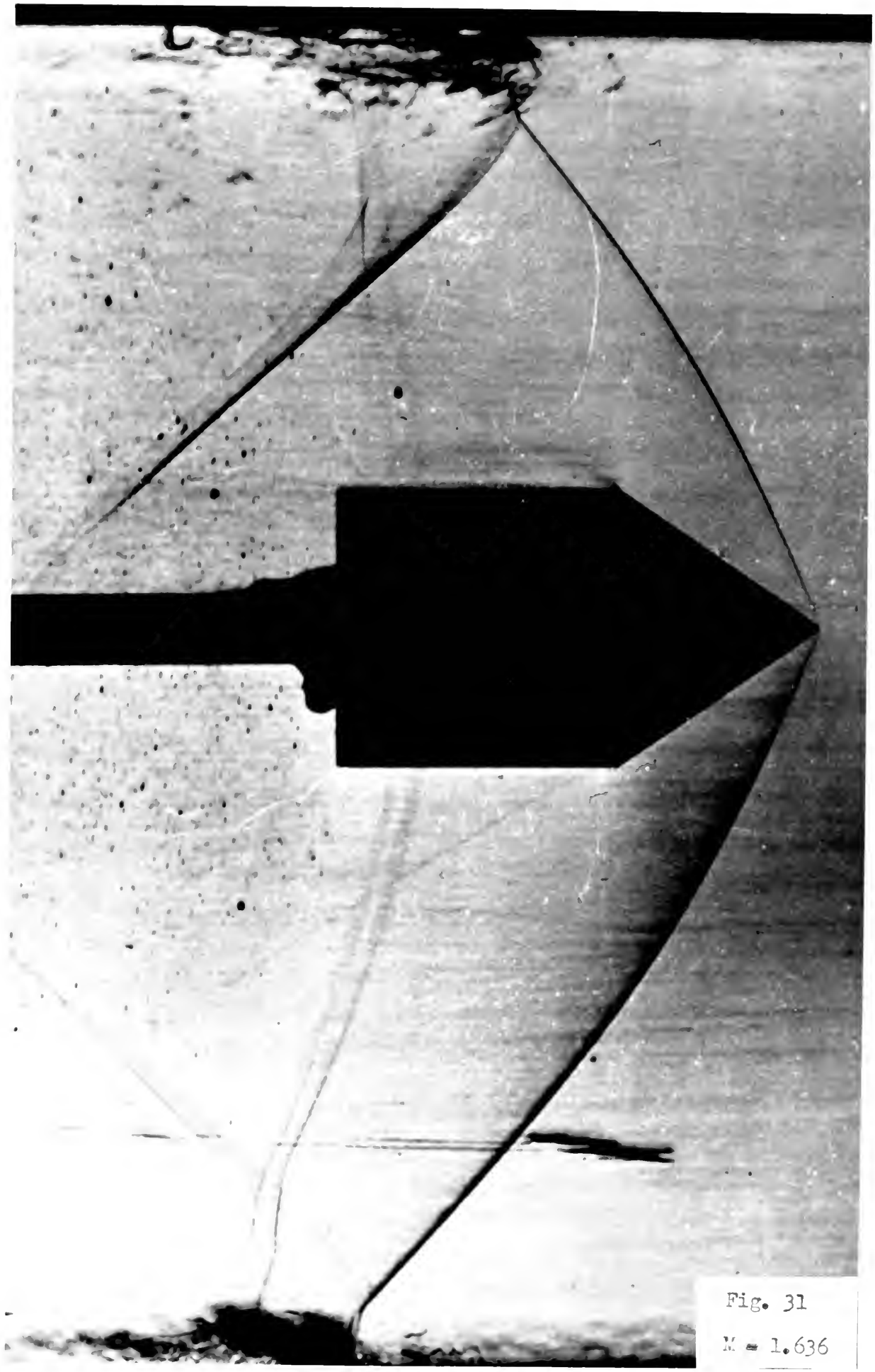

Fig. 31

M = 1.636

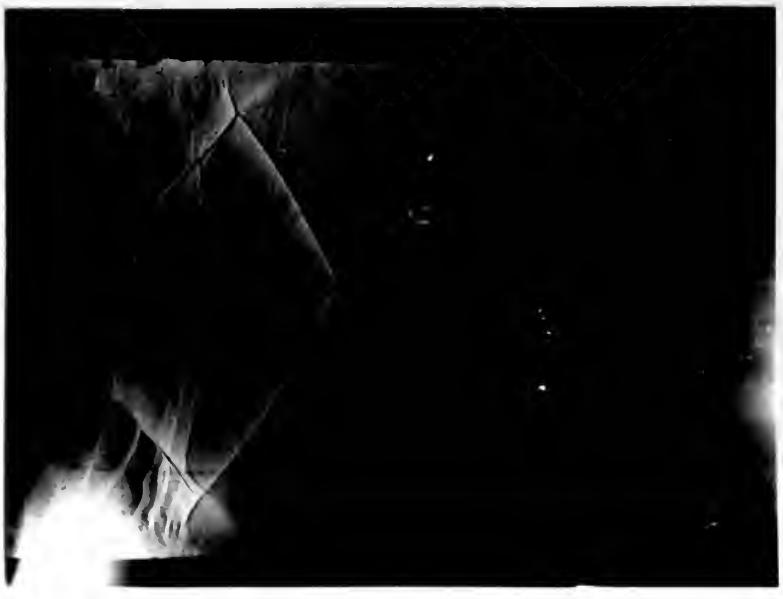

Fig. 32a

M = 1.694

Fig. 32b

M = 1.694

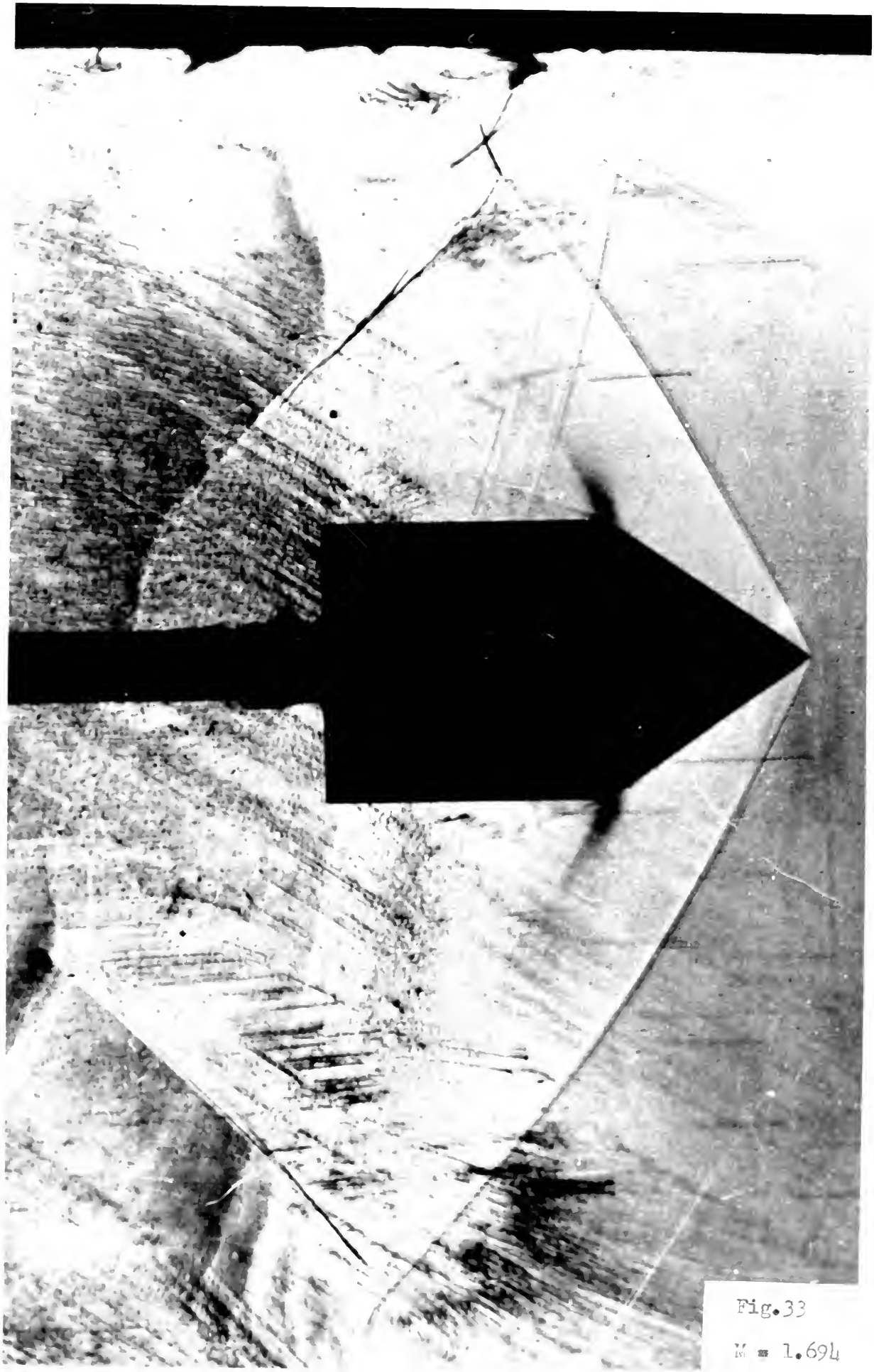

Fig.33

M = 1.694

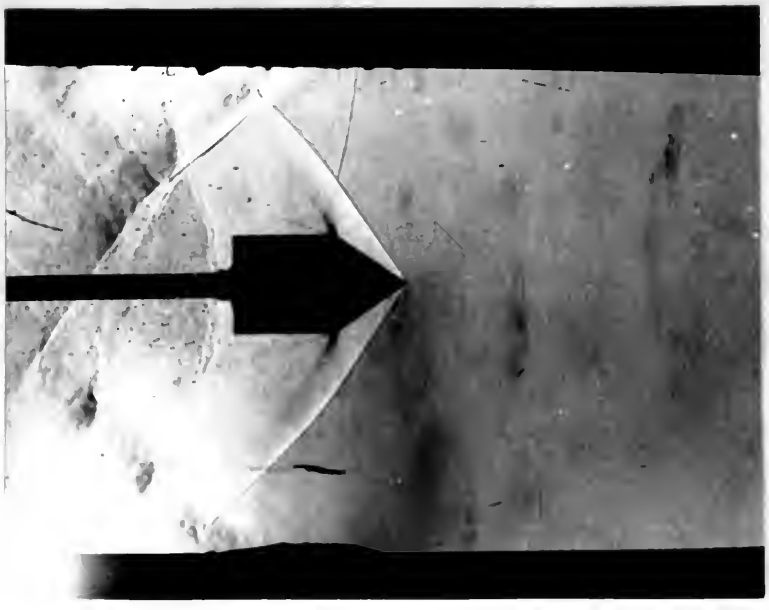

Fig. 34a

M = 1.86

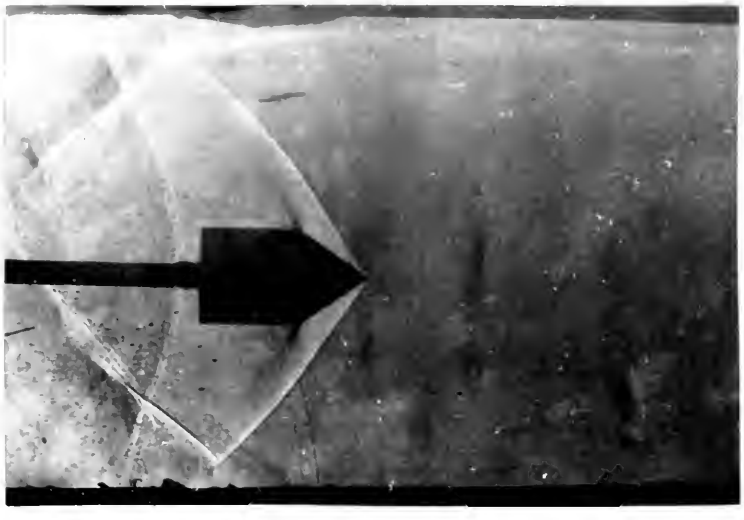

Fig. 34b

M = 1.76

Fig. 35a

M = 1.997

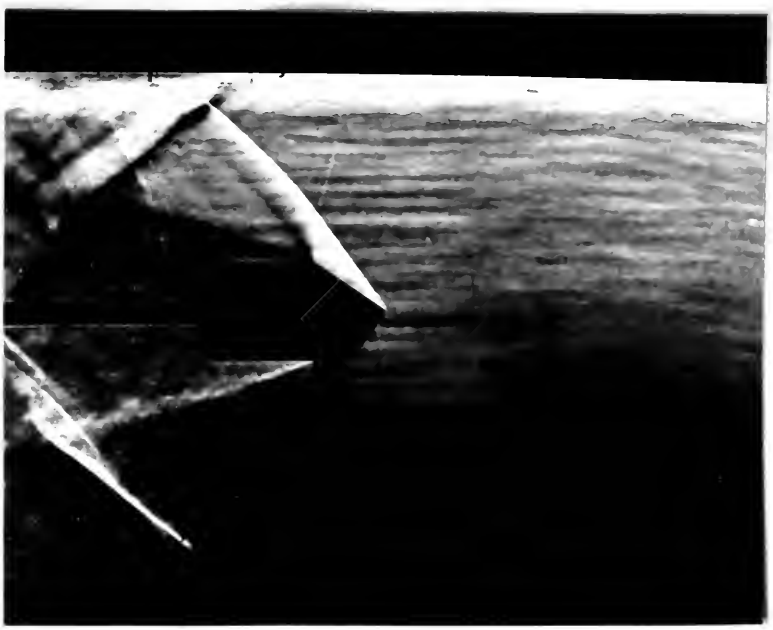

Fig. 35b

M = 1.997

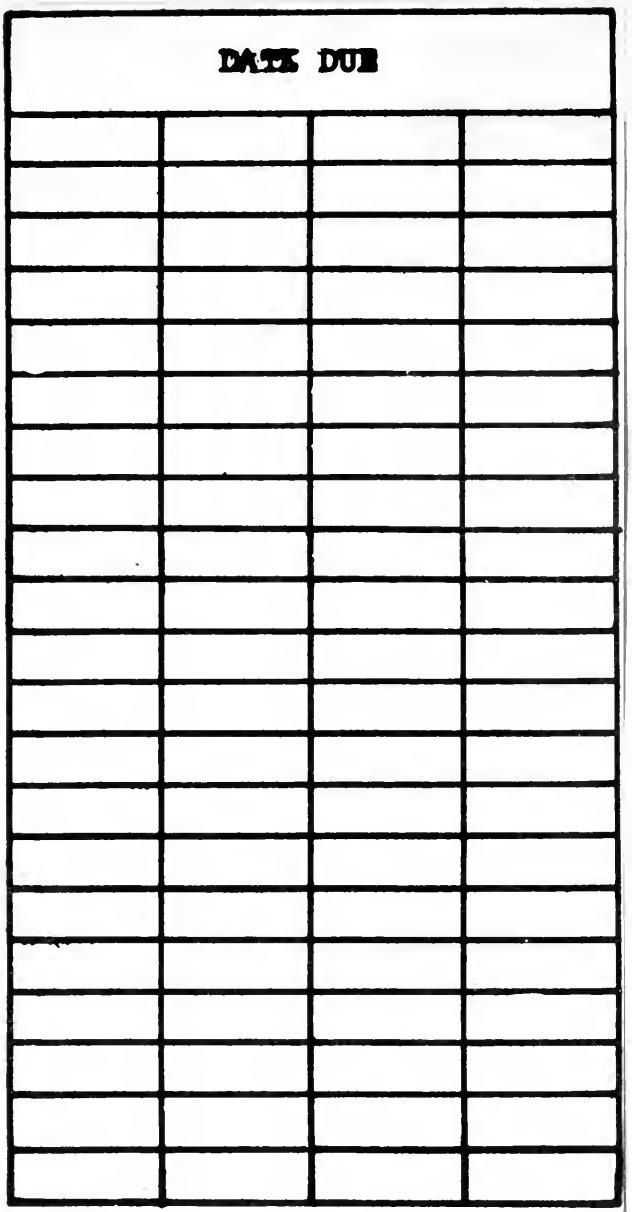
DATE DUE